Zanclean/Piacenzian transition on Cyprus (SE Mediterranean): calcareous nannofossil evidence of sapropel formation

M. Athanasiou, M. V. Triantaphyllou, M. D. Dimiza, A. Gogou & G. Theodorou

Geo-Marine Letters
An International Journal of Marine Geology

ISSN 0276-0460

Geo-Mar Lett
DOI 10.1007/s00367-015-0414-6

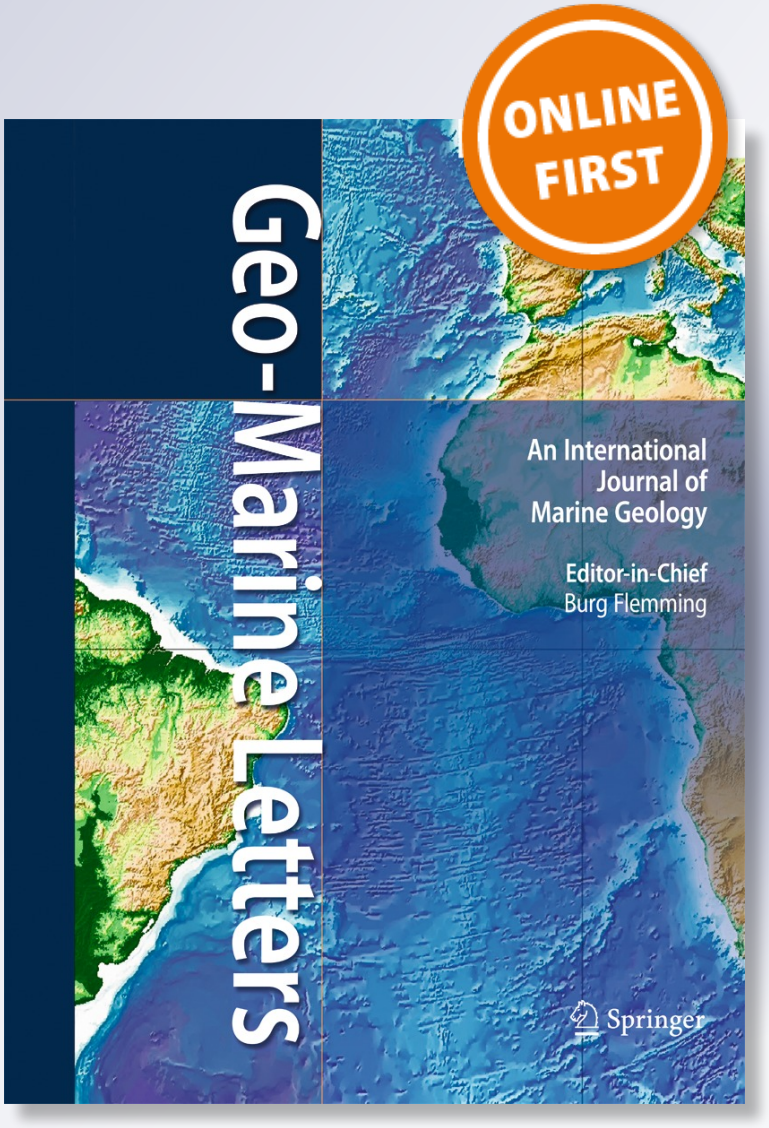

Springer

Geo-Mar Lett
DOI 10.1007/s00367-015-0414-6

ORIGINAL

Zanclean/Piacenzian transition on Cyprus (SE Mediterranean): calcareous nannofossil evidence of sapropel formation

M. Athanasiou[1] · M. V. Triantaphyllou[1] · M. D. Dimiza[1] · A. Gogou[2] · G. Theodorou[1]

Received: 27 February 2015 / Accepted: 16 July 2015

Abstract Quantitative analyses of calcareous nannofossils in the sediments of Pissouri South section on the island of Cyprus have produced a paleoceanographic record reflecting the paleoclimatic conditions during the Zanclean/Piacenzian transition. Pissouri South cyclical lithological alternations between organic-rich laminated layers and grey marls reflect the Earth's orbital precession. According to the calcareous nannofossil biostratigraphy which has been performed, the studied section is correlated with MNN14/15 and MNN16 calcareous nannofossil biozones and is astronomically dated between 4.065 and 3.217 Ma. Intervals of increased organic carbon content, along with the positive values of *Florisphaera profunda*, *Helicosphaera sellii*, *Discoaster* spp. and the subsequent increase of stratification S-index, correspond to the sapropel deposition during periods of wetter climate and intense continental runoff, especially from the river Nile. These layers alternate with grey marly intervals, featured by the increased values of small placoliths of *Reticulofenestra* and *Gephyrocapsa* species, which are indicative of eutrophic conditions during intense surface-water mixing. Our data support the prevalence of a generally warm phase characterized by the absence of high-frequency climate variations in the southeastern Mediterranean during the Zanclean/Piacenzian (Early/Late Pliocene) transition.

Introduction

One of the most critical periods in Earth's history spans the Pliocene Epoch, during which climatic and oceanographic conditions experienced a profound transition from relatively warm to cooler climate that heralded the high-magnitude glacial–interglacial oscillations of the Pleistocene Epoch. The latter resulted in the expansion of the Northern Hemisphere Ice Sheets (NHIS) at ~2.7 to 3.0 Ma (e.g., Marlow et al. 2000; Lisiecki and Raymo 2007) and the Middle Pleistocene Transition (MPT) at~0.8 to 1.2 Ma (e.g., Clark et al. 1999; Head and Gibbard 2005). Early/Late Pliocene transition (3.6–3.0 Ma) is considered as the last sustained interval when global climate was warmer than today (Ravelo et al. 2007; Brierley et al. 2009; LaRiviere et al. 2012; De Schepper et al. 2013). In fact, during 3.3–3.0 Ma, a period also inferred as the mid-Piacenzian Warm Period (mPWP) (e.g., Dowsett et al. 2012; Haywood et al. 2013), sea surface temperatures were characterized by increased values of ~3 °C (Haywood and Valdes 2004), while CO_2 concentrations were as high as the modern anthropogenic values of 400 ppm (Pagani et al. 2009; Bartoli et al. 2011). However, this warm period was interrupted by short-lived cooling episodes (e.g., Lisiecki and Raymo 2005) reflected in the gradual North Atlantic sea surface temperature decline, which culminated within the glacial Marine Isotope Stage MIS M2 at c. 3.3 Ma (e.g. Naafs et al. 2010).

Throughout the Miocene to Recent, eastern Mediterranean sedimentary sequences reflect oceanographic and climatic conditions that have undergone considerable variations; therefore, it represents one of the best disposed areas for Pliocene climatic reconstructions (e.g., Suc et al. 1995). Since the

Electronic supplementary material The online version of this article (doi:10.1007/s00367-015-0414-6) contains supplementary material, which is available to authorized users.

✉ M. Athanasiou
mairyatha@hotmail.com

[1] Faculty of Geology and Geoenvironment, University of Athens, 157 84 Panepistimioupolis, Athens, Greece

[2] Hellenic Centre for Marine Research, Institute of Oceanography, Anavyssos, 190 13 Attiki, Greece

Published online: 20 August 2015

closure of the Levantine–Arabian connection in the Early Miocene (e.g., Rohling et al. 2009), the only connecting point of the Mediterranean to the open sea (Atlantic Ocean) was to the west, through the Strait of Gibraltar. Isolation of the Mediterranean during late Miocene triggered the deposition of massive evaporates during the Messinian Salinity Crisis (e.g., Hsü et al. 1977). The subsequent tectonic opening of the Strait of Gibraltar (Rohling et al. 2009) followed by flooding from the Atlantic (e.g., Hsü et al. 1977) in the early Pliocene, resulted in the re-establishment of marine conditions, with deposition of cyclic bedded diatomites, marls, and carbonates (e.g., Hsü et al. 1977; Blanc-Valleron et al. 1998; Rouchy et al. 2001; Soria et al. 2008). Based on the extensive studies of Hilgen (1991a, b) and Hilgen et al. (1995, 2000), it is now accepted that the high frequency alternations of different lithologies, recognized throughout several Mediterranean land-based sedimentary sequences, are astronomically originated. The Zanclean "Trubi Formation" in Sicily and Southern Italy is such an example where the marly layers of the sequence (considered as the so-called sapropel "equivalent") reflect the periodicity of the Earth's precession cycle (e.g., Hilgen 1991a, b; Thunell et al. 1991a, b; Lourens et al. 1996). Interestingly, the ~23-kyr precession periodicity that is mainly influencing lower latitude monsoonal activity (Kroon et al. 1998), led to sapropel formation in the eastern Mediterranean Basin. These precession-controlled dark-colored, organic-rich layers (Rossignol-Strick 1983, 1985; Hilgen 1991a, b; Lourens et al. 1992) are interpreted to reflect the influence of the African monsoon activity, related with changes in sea surface productivity and salinity (Rossignol-Strick 1985; Kallel et al. 1997; Emeis et al. 2003). In fact, sapropels respond to periods of enhanced freshwater flux (e.g., Rohling and Hilgen 1991; Bar-Matthews et al. 2000; Kallel et al. 2000) during periods of strong summer insolation (e.g., Rohling 1994; Rohling et al. 2002; Meyers 2006). Evidence from eastern Mediterranean Quaternary sapropel studies indicate that freshwater stratification and organic carbon accumulation took place due to both enhanced productivity and hypoxia, during warm and wet climatic conditions (e.g., De Lange and Ten Haven 1983; Emeis et al. 2000a; Casford et al. 2003; Gogou et al. 2007; De Lange et al. 2008; Kuhnt et al. 2008; Triantaphyllou et al. 2009a, b, 2010, 2013; Katsouras et al. 2010; Schmiedl et al. 2010; Kouli et al. 2012; Triantaphyllou 2014).

Calcareous nannofossils are one of the most important pelagic sediment micro-components (Müller 1985; De Kaenel and Villa 1996; Castradori 1998; Negri et al. 1999a, b; Negri and Villa 2000; Vázque et al. 2000), used mainly for biostratigraphy and paleoceanographic reconstructions. Calcareous nannofossil biostratigraphy historically provides first-order age control in many outcrops and cores. However, the fluctuation patterns of calcareous nannofossil assemblages are also indicative of the group's quick response to oceanographic changes primarily involving temperature, salinity, primary production, and water stratification variations (e.g., Sierro et al. 1993, 2003; Erba 1994; Flores et al. 2003, 2005; Fenner and Di Stefano 2004; Triantaphyllou et al. 2004; Dimiza et al. 2008; Malinverno et al. 2009; Di Stefano and Sturiale 2010; Di Stefano et al. 2010, 2015; Erba et al. 2010; Patruno et al. 2015).

The geographical position of Cyprus in the southeastern Mediterranean Basin, under high latitude obliquity and mid-low latitude precessional influence, provides an ideal area for the interpretation of paleoceanographic records (e.g., Emeis et al. 1998; Waters et al. 2010). Pissouri Basin, at the southwesterrn part of the island, has been exhaustively studied during the last decades, particularly for the exposed Messinian deposits (e.g., Rouchy et al. 2001; Krijgsman et al. 2002; Kouwenhoven et al. 2006; Morigi et al. 2007; Bison et al. 2009). A preliminary description of the Zanclean/Piacenzian sequence in Pissouri Basin (Pissouri South section) has been provided by Triantaphyllou et al. (2010), revealing rhythmic sapropelic formation during this interval. There is however, a lack of detailed information regarding the Zanclean/Piacenzian transition in this part of the Mediterranean, particularly with regard to a well-established record of paleoceanographic-paleoclimatic changes. To achieve this goal, we have performed micropaleontological (calcareous nannofossils) and geochemical (organic carbon content, OC) analyses, in the sediments of Pissouri South section, in order (1) to analyze the calcareous nannofossil assemblages and their relationship with lithology, and (2) to refine the paleoceanographic–paleoclimatic conditions during the Zanclean/Piacenzian transition in this part of the Mediterranean.

Geological setting

Located within the Levantine Basin, the island of Cyprus is considered as a part of a northward–dipping subduction zone (Cyprean Arc) that extends between southern Cyprus and the Eratosthenes Seamount (Fig. 1), at the northern margin of the African Plate (Payne and Robertson 1995; Harrison et al. 2004). Since the early Mesozoic, this complex tectonic zone has produced an array of four tectonostratigraphic terrains, which during Late Oligocene times became uplifted forming the basement of four sedimentary basins; Polemi, Pissouri, Limassol, and Psematismenos. These were active in the Late Miocene–Early Pliocene (Payne and Robertson 1995). The Pissouri Basin corresponds to a small NNW–SSE tectonic depression, consisting of Pliocene–Pleistocene deposits of the Nicosia Formation. The Nicosia Formation sedimentary units (Fig. 2) represent a significant shift towards deeper water

facies during the Early Pliocene (Robertson et al. 1991; Foucault and Mélières 2000; Bertoni and Cartwright 2007; Soria et al. 2008). They comprise a complex assemblage of clastic, marine depositional facies that contain grey and yellow siltstones alternating with layers of calcarenites and marls (Stow et al. 1995). The abrupt uplift of Troodos Massif, that occurred around ~2 Ma at the Plio–Pleistocene boundary (Stow et al. 1995; Schirmer 2000) and continues up to the present day (e.g., Mc Callum and Robertson 1995), resulted in the deposition of fanglomerates at the top of the Pissouri Basin sequence (Waters et al. 2010) (Fig. 2).

Material and methods

Pissouri South section

Pissouri South section, located at the southwestern edge of the Pissouri Basin, is 152 m high and consists of rhythmically laminated marls, marly sands, silty sands, and sandstones of the Nicosia Formation (Fig. 2). The first 44 m of the section display 62 alternations of laminated light yellowish brown layers, 30–60 cm thick, alternating with light grey marls, 70 cm–2.5 m thick (Fig. 3a–c). Similar lithological features

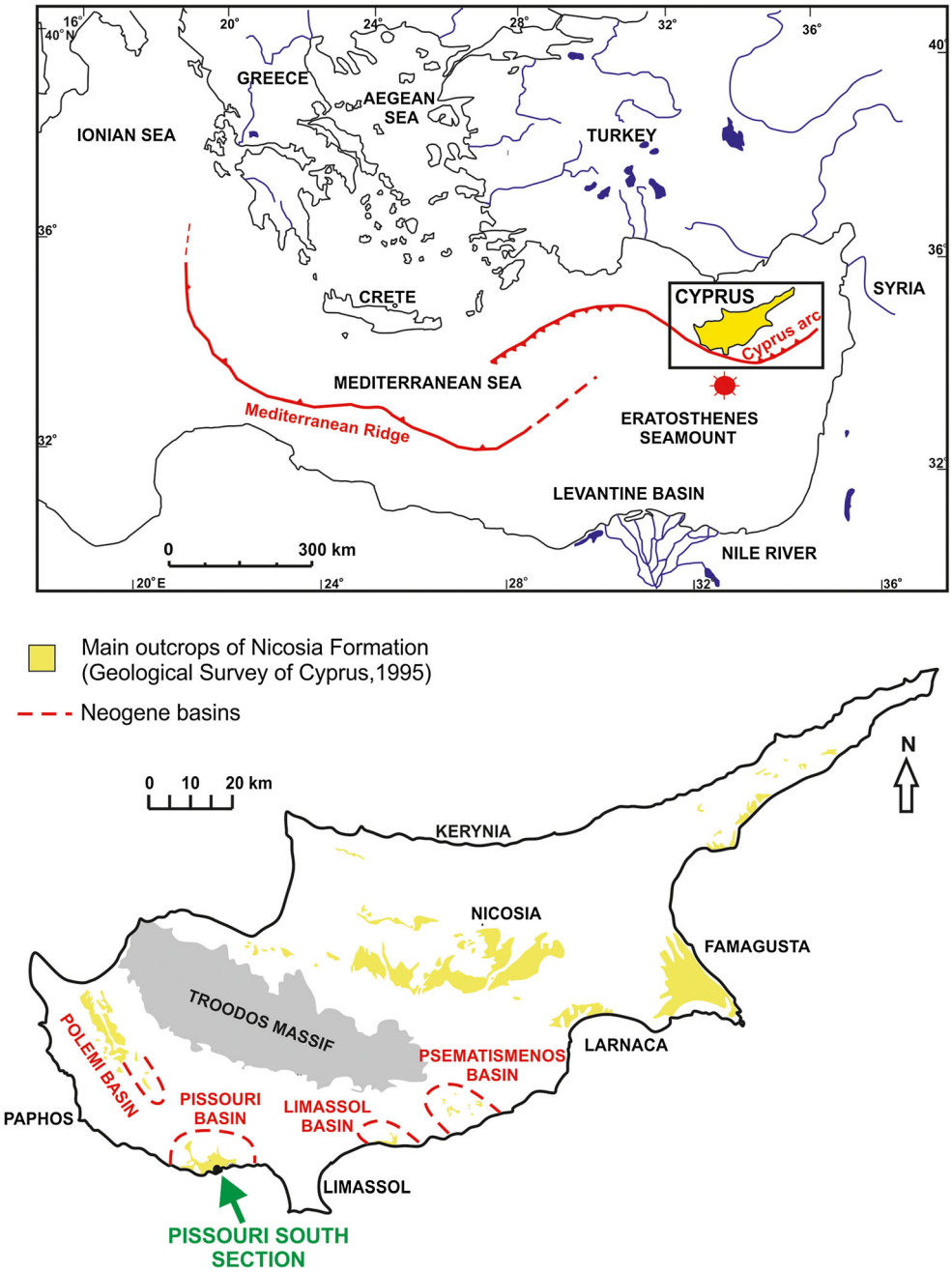

Fig. 1 Map of the eastern Mediterranean and northern Levantine Sea, showing the location of Pissouri South section on the island of Cyprus

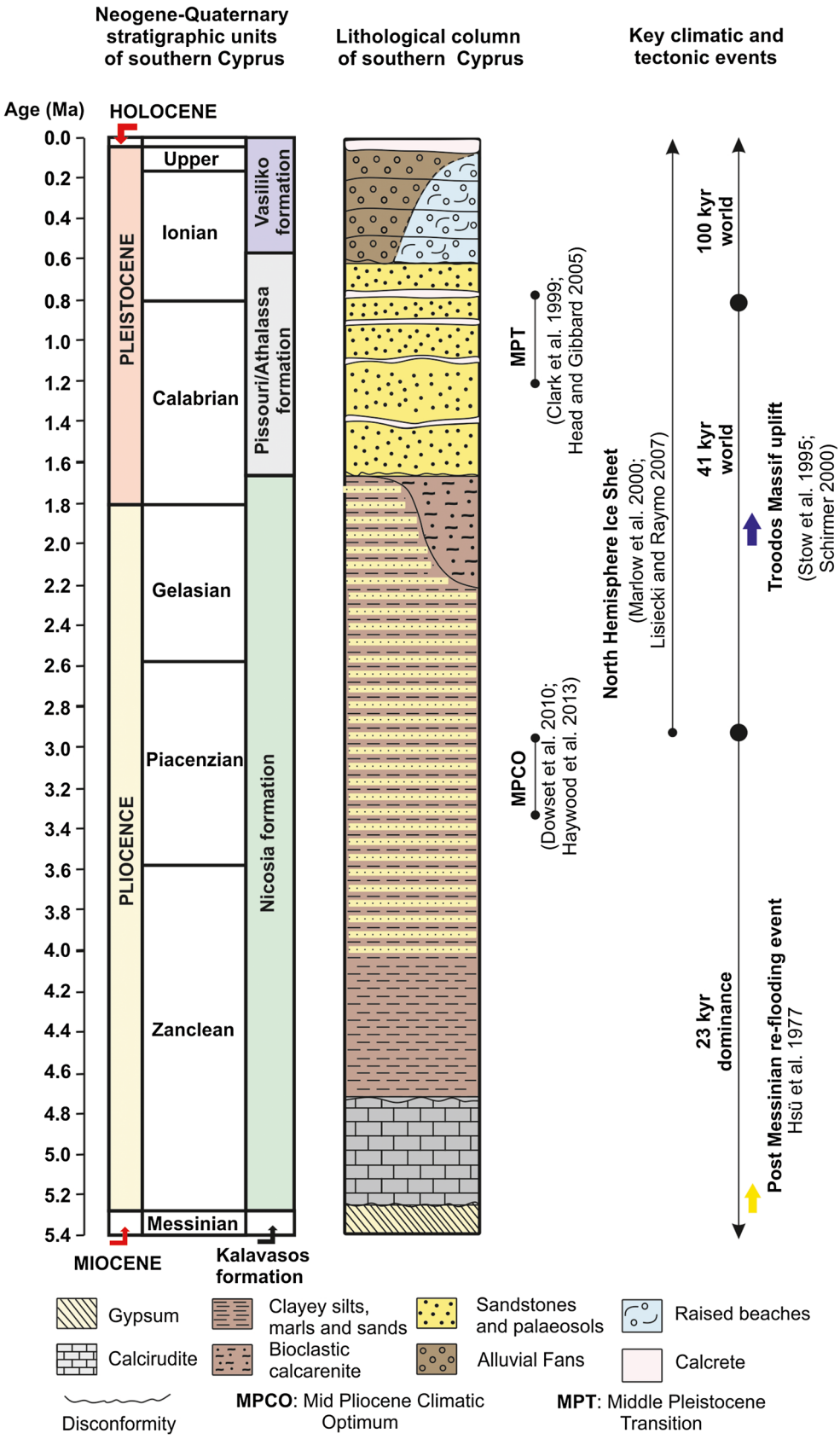

Fig. 2 Generalized lithostratigraphy and chronostratigraphy of southern Cyprus stratigraphic units and the main tectonic and climatic events (modified from Waters et al. 2010)

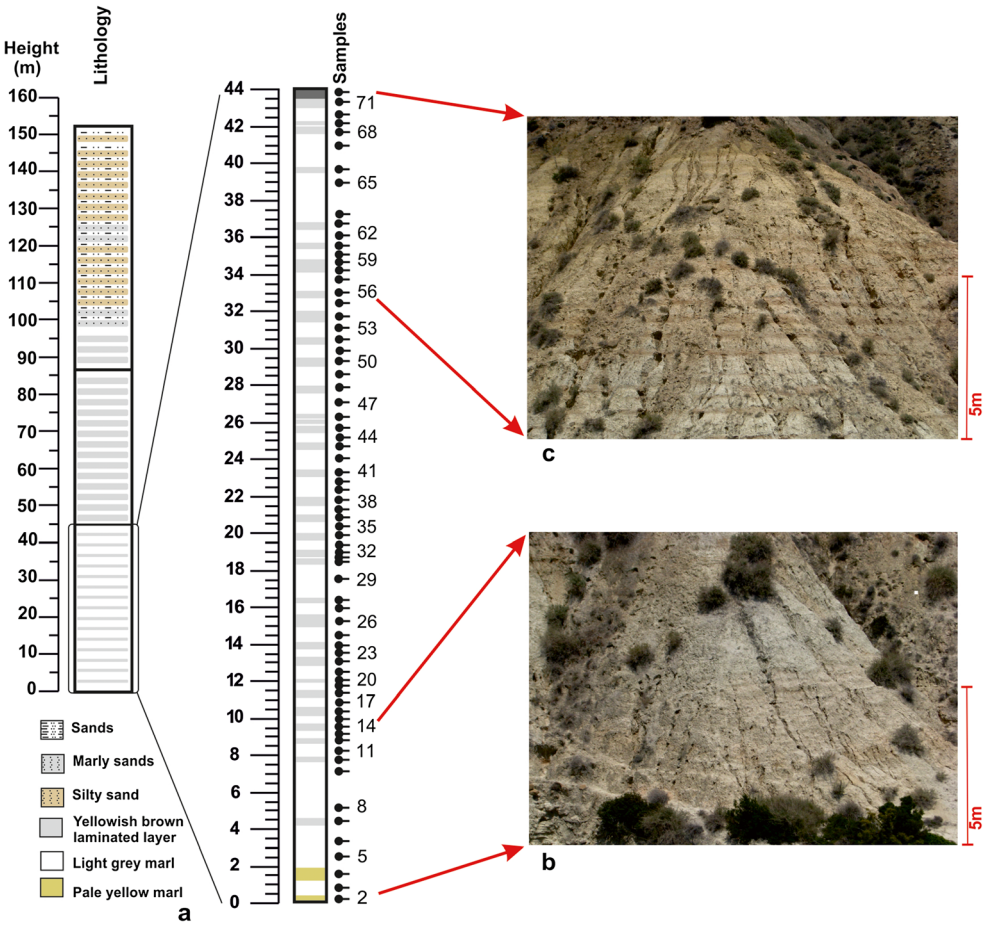

Fig. 3 **a** Lithology of Pissouri South sediments and detailed logging of the lower part of the section. **b**, **c** The lower and upper part of the section, displaying prominent lithological alternations between yellowish brown laminated layers and grey marls

characterize the following 42 m of the section, but the laminated beds become gradually rarer and considerably thicker (Fig. 3a). The last 66 m contain multiple grey to brown marly layers that upwards are replaced by marly sands alternating with sands and silty sands (Fig. 3a). Logging and sampling of the entire section was performed during summer 2005 and accomplished through collaboration between the University of Athens and the Geological Survey of Cyprus. In the present study, we have analyzed the lower 44 m of the section, with an average sampling resolution of 10–20 cm within the laminated layers and 40–80 cm in the marly intervals (Fig. 3b, c); from each layer one or two samples (base and top) have been collected depending on the layer thickness. The weathered surface was cleaned and only fresh material was sampled; in total 72 samples (samples P1/1-P1/72) have been studied from the considered part of the section. A simple spectral analysis (using the program Past.exe) has been applied to the collected lithostratigraphic data.

Organic carbon content analysis

Organic carbon (OC) contents were determined in 72 freeze-dried and homogenized samples which were initially decarbonated using repetitive additions of HCl (25 %, v/v), separated by 60 °C drying steps, until no effervescence was observed. Organic carbon was then determined by combustion in an oxygen atmosphere, and the produced carbon dioxide was quantitatively measured using a Flash 2000 Elemental Analyzer. The analytical precision was in the order of ±0.02 %. Organic carbon (OC) analysis was performed at the Hellenic Centre of Marine Research.

Calcareous nannofossil analysis

The preparation of samples followed the standard smear slide techniques for calcareous nannofossil analysis (Perch-Nielsen 1985; Bown and Young 1998). All samples were routinely examined at 1,250×, using a LEICA DMLSP light microscope (LM). A scanning electron microscope analysis (SEM Jeol JSM 6360, Department of Historical Geology–Paleontology, University of Athens) has been used for taxonomical purposes. Total assemblage composition was evaluated in a first count, in which all specimens (coccoliths/nannoliths) were counted until a statistically significant total of at least 500 nannofossils had been obtained. A second count was performed from

additional 15 fields of view for the less common taxa, with abundances <2 % in the first count. Taxonomic concepts of the considered taxa follow Perch-Nielsen (1985), Aubry (1984, 1988, 1989, 1990, 2014), and Bown and Young (1998). For the biostratigraphic assignment of the Pissouri South section, frequencies of index species, mainly represented by *Discoaster asymmetricus*, *Discoaster tamalis*, *Discoaster surculus*, *Discoaster pentaradiatus*, *Discoaster brouweri* , and *Discoaster variabilis*, were established in counts of 50 discoasterids following the methods and determination of the biostratigraphic events described by Rio et al. (1990) and Backman et al. (2012). Biozonation is after Rio et al. (1990) and biochronology follows Lourens et al. (2004) and Raffi et al. (2006), as both schemes provide biohorizon ages especially for the eastern Mediterranean. Stage ages used are after Gradstein et al. (2004, 2012). We applied the ratio between *Florisphaera profunda* (F), small *Gephyrocapsa* spp. <3 μm (sG) and small *Reticulofenestra* spp. <5 μm (sR; mostly *R. minuta* and *R. minutula*) abundances: S=F/(F+sG+sR) as stratification index (modified from Flores et al. 2000; Triantaphyllou et al. 2009b). The increase in S values indicates gradual establishment of stratified conditions in the water column and the onset of a nutrient-rich environment in the deep photic zone (Triantaphyllou et al. 2009b; Triantaphyllou 2014). Following Palumbo et al. (2013) and Triantaphyllou (2014), the sum of the warm upper-photic zone (UPZ) taxa of Rhabdosphaeraceae family mostly represented by *Rhabdosphaera clavigera* and *Discosphaera tubifera*, *Syracosphaera* spp. (mostly *S. pulchra*), *Umbilicosphaera* spp. (mostly *U. jafari*), *Pontosphaera* spp., *Umbellosphaera tenuis*, and *Calciosolenia* spp. is used as a proxy of warm and oligotrophic surface waters, in accordance with their ecological preferences.

Results

Organic carbon content

Organic carbon (OC) content in all laminated layers of Pissouri South section is characterized by higher values, up

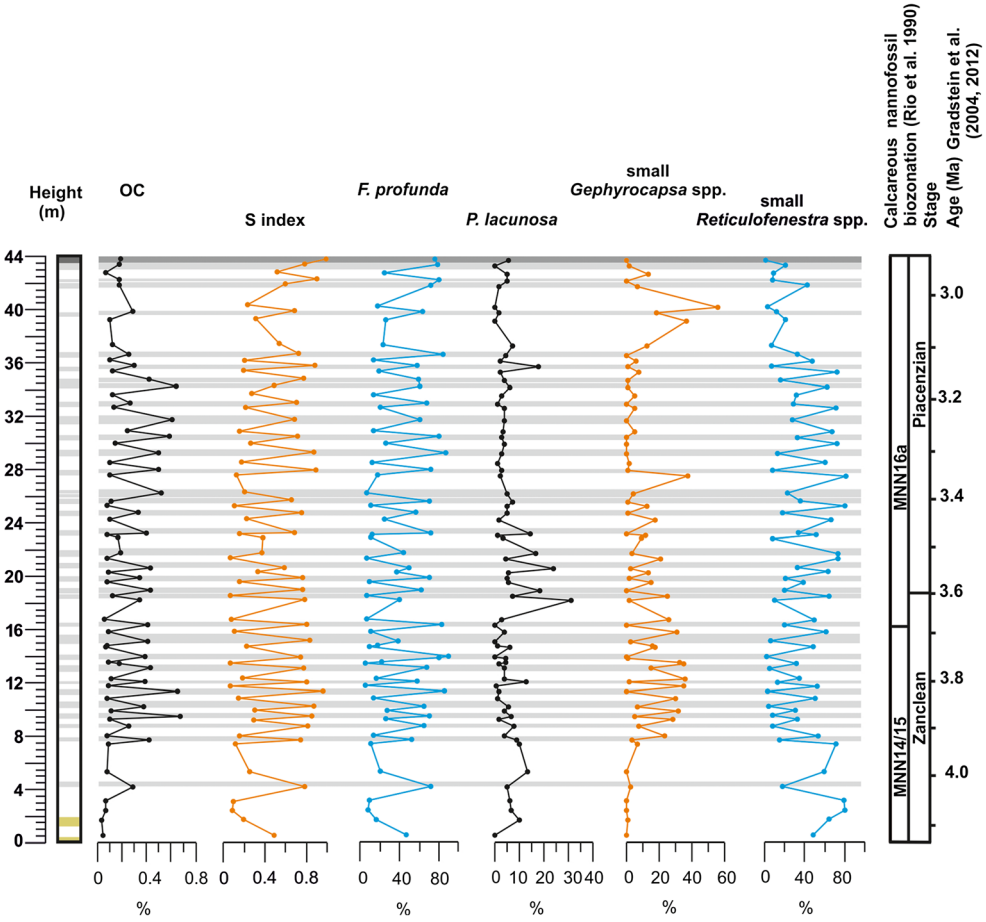

Fig. 4 Organic carbon content (OC %), S index distribution and dominant calcareous nannofossil species relative abundances, counted in 500 nannofossil specimens. Sapropelic layers are highlighted in *grey bands*

to ~0.6 %, while a significant drop has been observed in the light grey marly layers down to ~0.04 % (Fig. 4). Pissouri South Pliocene sapropelic layers display reasonable OC content, similar to Capo Rossello, Punta Piccola (Beltran et al. 2007).

Calcareous nannofossil assemblages

Calcareous nannofossils are abundant and generally very well-preserved in all samples. The comparatively good preservation potential of most heterococcoliths has been assessed

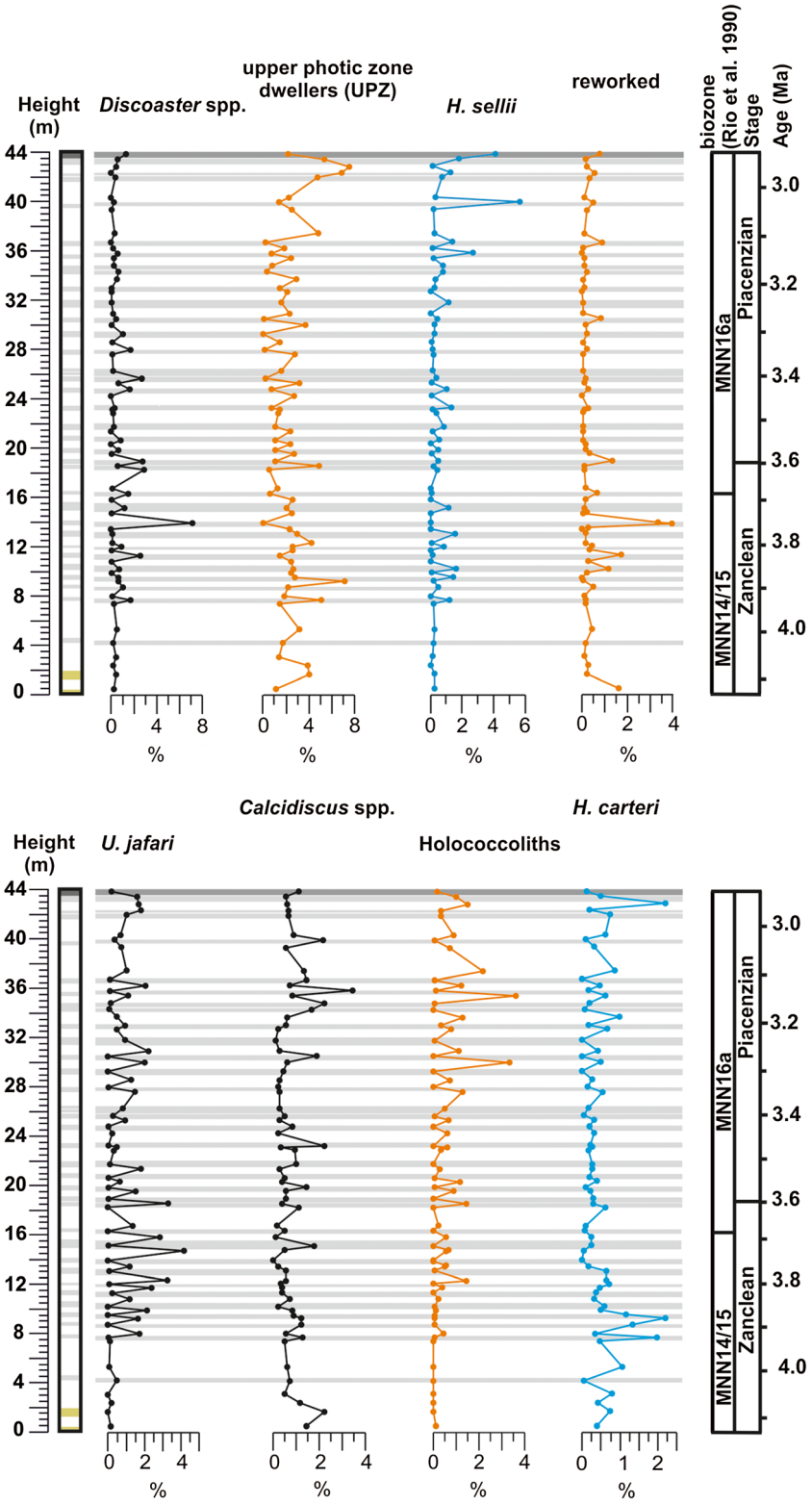

Fig. 5 Minor calcareous nannofossil species relative abundances in 500 nannofossil specimens. Sapropelic layers are highlighted in *grey bands*

by different works (e.g., Roth and Coulbourn 1982; Castradori 1993); therefore, the investigated nannofossil assemblages are considered representative of the water column conditions. Species are listed alphabetically in a taxonomic list supplied in the electronic supplementary material available online for this article. Trends of representative taxa are plotted in Figs. 4, 5, and 6. *Florisphaera profunda* is the dominant species of the assemblage both in absolute and relative abundances, reaching values up to 90 % within the increased OC laminated layers. In contrast, maximum values of both small *Reticulofenestra* spp. <5 μm and small *Gephyrocapsa* spp. <3 μm have been reported in the low OC light grey layers. In particular, small *Reticulofenestra* spp. <5 μm exhibit values up to 81 %, showing evident decrement above 36.6 m. Maximum values of small *Gephyrocapsa* spp. <3 μm (55 %) have been observed between the heights of 37.3 m and 41.8 m. *Pseudoemiliania lacunosa* is characterized by continuous presence and abundances up to 31 %; an increase is observed between 18.2–23.2 m, coinciding with the slightly reduced values of small *Reticulofenestra* spp. at the same interval (Fig. 4). *Sphenolithus* spp. (*S. abies*, *S. neoabies*) are restricted in the lower part of the section, up to 20.6 m height; values do not exceed 10 % (Fig. 6). *Reticulofenestra pseudoumbilicus* >7 μm displays a similar distribution pattern, with the last representatives recorded at 15.8 m (Fig. 6). Values of *Helicosphaera sellii* do not exceed 12.5 % (Fig. 5), exhibiting a gradual increase above 35.7 m, while abundance peaks are observed in the laminated intervals. *Helicosphaera carteri* shows an opposite pattern, contributing with much lower values (Fig. 5). Warm upper photic zone species contribute with abundances up to 8 % (Fig. 5). Interestingly, *Umbilicosphaera jafari* and holococcoliths show increased values in the grey marly layers (Fig. 5). The *Discoaster* group exhibits low abundances (max 7.5 %; peaks observed mostly in the laminated layers), dominated by *D. asymmetricus* and *D. tamalis* (Fig. 6). *Discoaster asymmetricus* is characterized by continuous distribution above 7.7 m, whereas *D. pentaradiatus* follows a similar pattern except for a periodical absence in between 18.5 m and 24.2 m. *Discoaster tamalis* occurs with higher frequencies above 15.1 m height, with maximum value (72 % within the *Discoaster* group, Fig. 6) recorded at 30.4 m. Finally, the laminated marls are featured by increased values of S index up to 0.99, whereas grey layers exhibit maximum values of 0.54 (Fig. 4). Positive peaks of reworking species are also reported in laminated marls, reaching 3.6 % (Fig. 5).

Biostratigraphy, chronostratigraphy and sedimentation rates

Five main calcareous nannofossil biohorizons are recognized within the considered tract of the Pissouri South section (Fig. 6; main biostratigraphic indices are illustrated in Fig. 7):

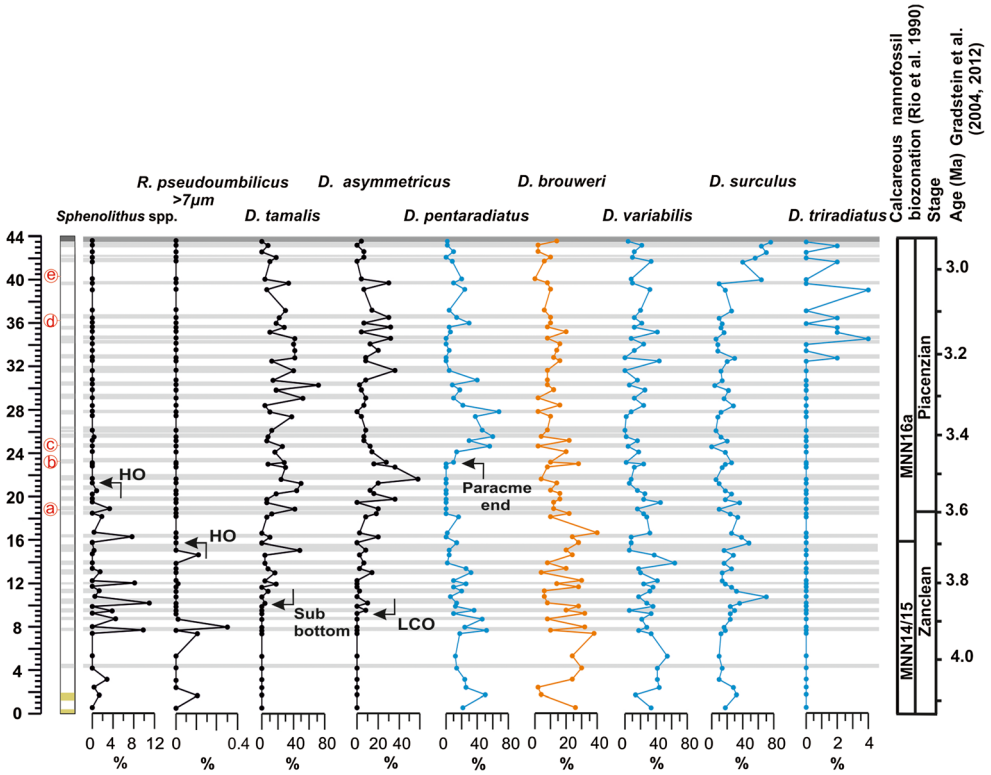

Fig. 6 Calcareous nannofossil biostratigraphic indices. Relative abundances of the various *Discoaster* species were established in counts of 50 discoasterids. *Sphenolithus* spp. and *Reticulofenestra pseudoumbilicus* were counted in 500 nannofossil specimens. *HO*: highest occurrence, *LCO*: lowest common occurrence, *LO*: lowest occurrence. Additional planktonic foraminiferal biohorizons (Triantaphyllou et al. 2010) are shown on the left: (a) *Globorotalia margaritae* HO, (b) *Globorotalia crassaformis* LO, (c) *Globorotalia puncticulata* temporary disappearance, (d) *Globorotalia crassaformis* reappearance, (e) *Globorotalia puncticulata* reappearance

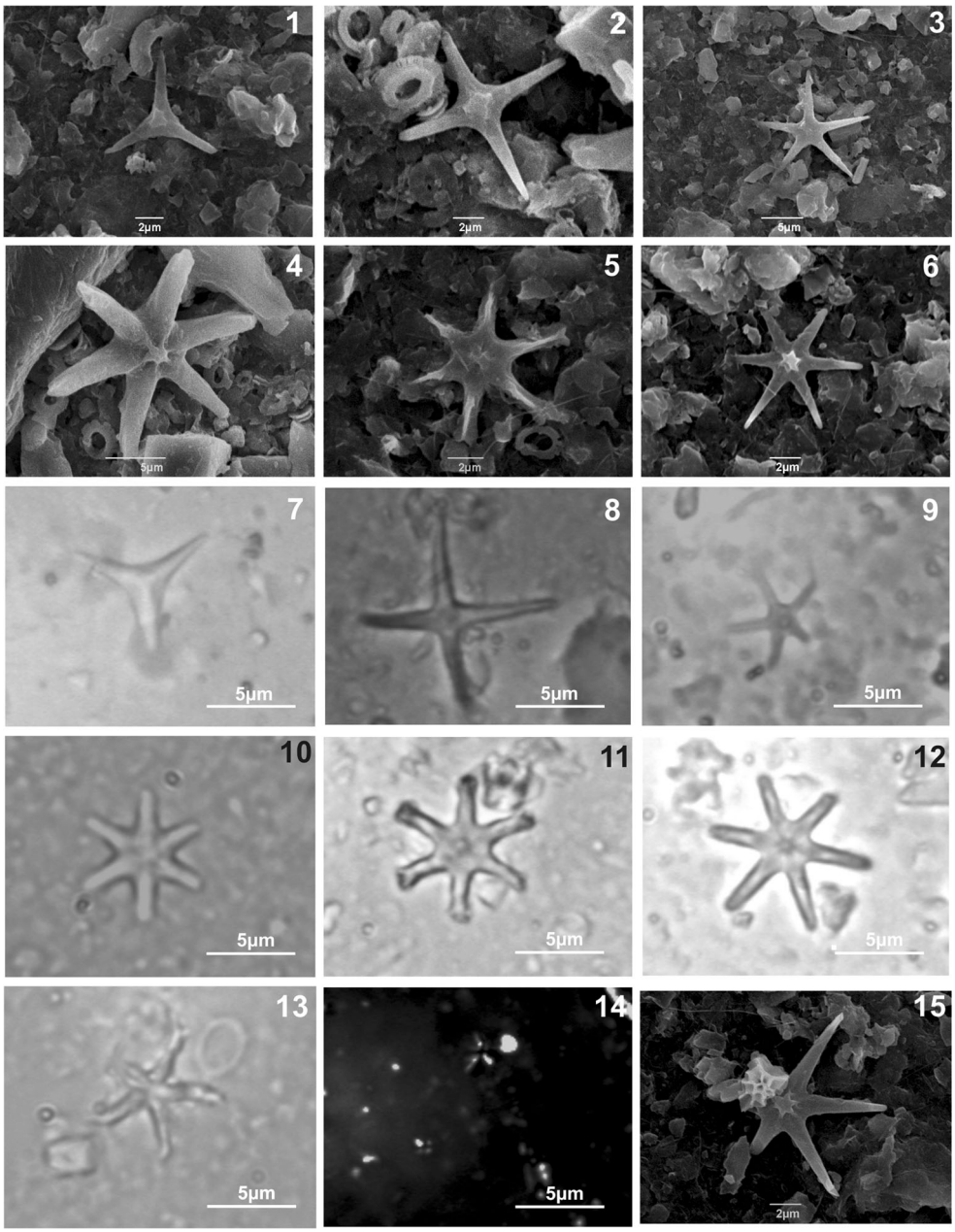

Fig. 7 Calcareous nannofossil biostratigraphic indices. **1** *Discoaster triradiatus* (SEM image, sample P1/14). **2** *Discoaster tamalis* (SEM image, sample P1/34). **3** *Discoaster asymmetricus* (SEM image, sample P1/14), **4** *Discoaster surculus* (SEM image, sample P1/14). **5** *Discoaster variabilis* (SEM image, sample P1/14). **6** *Discoaster brouweri* (SEM image, sample P1/14). **7** *Discoaster triradiatus* (LM image, sample P1/14). **8** *Discoaster tamalis* (LM image, sample P1/34). **9** *Discoaster asymmetricus* (LM image, sample P1/14). **10** *Discoaster surculus* (LM image, sample P1/14). **11** *Discoaster variabilis* (LM image, sample P1/14). **12** *Discoaster brouweri* (LM image, sample P1/14). **13** *Discoaster pentaradiatus* (LM image, sample P1/67). **14** *Sphenolithus abies* (LM image, sample P1/14). **15** *Sphenolithus abies* ontop of *D. brouweri* (SEM image, sample P1/14)

(1) The continuous presence of *D. asymmetricus* observed above 7.7 m of the section with relative frequencies exceeding 8 %, can be interpreted as the LCO (lowest common occurrence) of the species which according to Backman et al. (2012) is dated at 4.04 Ma in the late Zanclean.

(2) Upwards, at 10.2 m height of Pissouri South section, the abundance of *Discoaster tamalis* increases more than 4 %, corresponding to the subbottom *D. tamalis* bioevent (Lourens et al. 2004), which has been dated at 3.97 Ma for the eastern Mediterranean (Lourens et al. 2004). Although not used in existing biostratigraphic schemes (e.g., Raffi et al. 2006; Backman et al. 2012), the first appearance of *D. tamalis* is nonetheless useful in the biostratigraphic analysis of late Zanclean deposits (Rio et al. 1990).

(3) *Reticulofenestra pseudoumbilicus* is absent above 15.8 m height, defining the *R. pseudoumbilicus* HO (highest occurrence) biohorizon, which also marks the boundary between MNN14/15 and MNN16 biozones (Rio et al. 1990). The recognized biohorizon is equivalent to the NN14/15–NN16 (Martini 1971) and CNPL3–CNPL4 (Backman et al. 2012) biozones boundary, with an age confirmed for the eastern Mediterranean at 3.84 Ma in the late Zanclean (Lourens et al. 2004; Raffi et al. 2006) or 3.82 Ma (Backman et al. 2012).

(4) *Sphenolithus* spp. HO is observed above the disappearance of *R. pseudoumbilicus*, at 20.6 m height. *Sphenolithus* spp. HO at the lower part of NN16 is dated at 3.7 Ma for the eastern Mediterranean (Raffi et al. 2006).
(5) The absence of the otherwise frequent species *D. pentaradiatus* in between 21.7–23.1 m correlates with the *D. pentaradiatus* paracme zone (Driever 1981) at the lower part of NN16. Rio et al. (1990) considered the beginning and the end of this interval useful for very fine biostratigraphic subdivision, as they were observed in several eastern Mediterranean sections. The top of *D. pentaradiatus* paracme nannofossil bioevent is placed at 23.1 m in the Pissouri South section, thus providing an age of 3.61 Ma (Lourens et al. 2004) that approximates the base of the Piacenzian Stage (3.60 Ma; Gradstein et al. 2004, 2012).

Additional planktonic foraminiferal bioevents recognized in Triantaphyllou et al. (2010) are used for strengthening the biostratigraphic assignment of Pissouri South section (Fig. 6): (a) *Globorotalia margaritae* HO (3.81 Ma; Lourens et al. 2004), (b) *Globorotalia crassaformis* LO (lowest occurrence) marking the Zanclean/Piacenzian boundary (3.60 Ma, Lourens et al. 2004), (c) *Globorotalia puncticulata* temporary disappearance (3.57 Ma; Lourens et al. 2004), (d) *G. crassaformis* reappearance (3.35 Ma; Lourens et al. 2004), (e) *G. puncticulata* reappearance (3.31 Ma; Lourens et al. 2004).

Based on the defined biohorizons within Pissouri South section, sedimentation rates have been calculated between 4.04–3.97 Ma (7.7–10.2 m) as 3.3 cm/kyear, while between 3.97 and 3.84 Ma (10.2–15.6 m) values are slightly increased to 4.21 cm/kyear (Table 1). Within the interval from 3.84 to 3.81 Ma (15.8–18.5 m), sedimentation rates continue to increase to 9.0 cm/kyear; in between 3.81 and 3.7 Ma (18.5–20.6 m) values drop to 1.94 cm/kyear, before rising again to 2.28 cm/kyear within 3.7 and ~ 3.61 Ma (20.6–23.1 m). An evident increase has been observed between 3.6–3.57 Ma (21.3–24.7 m) with the sedimentation rates to exhibit values of 7.53 cm/kyear. Within the next 11.4 m of section spanning 3.57 to ~ 3.335 Ma (24.7 to 36.1 m) sedimentation rates decrease again to 4.8 cm/kyear, while the upper part of the section spanning period of 3.35–3.31 Ma (36.1–40.2 m) is characterized by a sharp increase, with sedimentation rates reaching maximum values of 11.25 cm/kyear (Table 1).

Discussion

Zanclean/Piacenzian sapropelic layers: paleoceanographic–paleoclimatic implications

The increase of the lower and mid photic zone dwellers *F. profunda* and *H. sellii*, along with the concomitant high values of S index (up to 0.99; Fig. 4) within the OC enriched laminated layers of Pissouri South section (Fig. 8), imply the gradual establishment of stratified conditions, the onset of increased productivity in a nutrient-rich deep photic zone, and the concomitant development of deep chlorophyll maximum (DCM), (Fig. 9). *Florisphaera profunda* is one of the dominant deep dwellers of the modern eastern Mediterranean water column during the warm season (e.g., Triantaphyllou et al. 2004; Malinverno et al. 2009); apparently abundant in the

Table 1 Defined biohorizons in the Pissouri South section and calculated sedimentation rates

Biohorizon	Position (m)	Thickness (m)	Age (Ma)	Duration (Ma)	Sedimentation rates (cm/kyear)
LCO *D. asymmetricus* subbottom *D. tamalis*	7.7 10.2	2.5	4.04 3.97	0.07	3.57
subbottom *D. tamalis* HO *R. pseudoumbilicus*	10.2 15.8	5.6	3.97 3.84	1.03	4.30
HO *R. pseudoumbilicus* HO *G. margaritae*	15.8 18.5	2.7	3.84 3.81	0.03	9.00
HO *G. margaritae* HO *Sphenolithus* spp.	18.5 20.6	2.1	3.81 3.7	0.11	1.90
HO *Sphenolithus* spp. top paracme *D. pentaradiatus*	20.6 23.1	2.5	3.7 3.61	0.09	2.78
LO *G. crassaformis* temporary disappearance *G. puncticulata*	23.1 24.7	1.6	3.60 3.57	0.03	5.33
temporary disappearance *G. puncticulata* reappearance *G. crassaformis*	24.7 36.1	11.4	3.57 3.35	0.22	5.18
reappearance *G. crassaformis* reappearance *G. puncticulata*	36.1 40.2	4.1	3.35 3.31	0.24	10.25

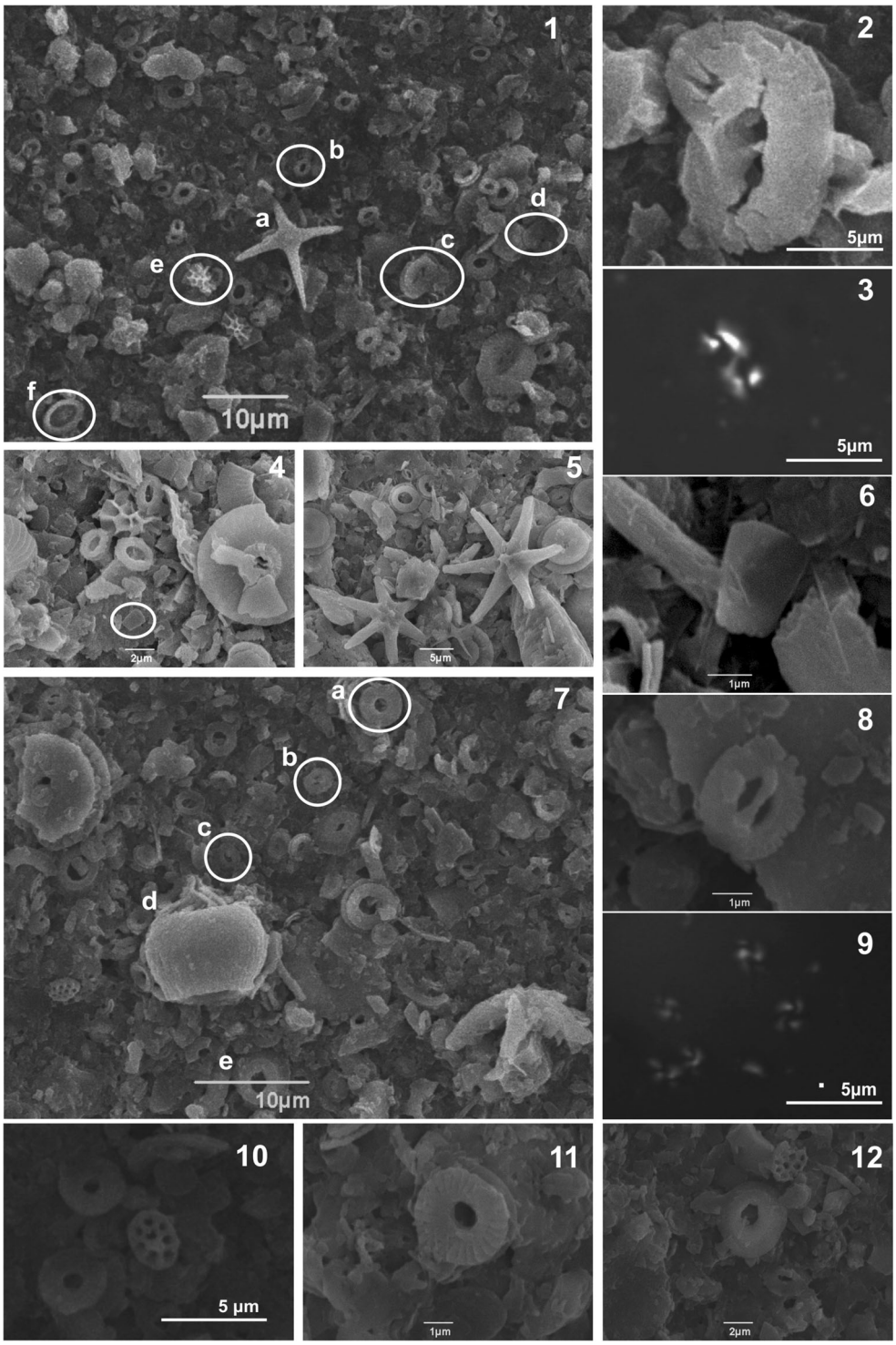

Fig. 8 **1**–**6** Typical calcareous nannofossil assemblage of the laminated brownish layers reflecting sapropelic conditions; the almost excellent preservation state is remarkable. **1** (SEM image, sample P1/34): *a Discoaster tamalis*, *b* small *reticulofenestra* spp., *c Helicosphaera sellii*, *d Florisphaera profunda*, *e Sphenolithus abies*, *f Syracosphaera pulchra*. **2** *Helicosphaera sellii* (SEM image, sample P1/14). **3** *Helicosphaera sellii* LM photo (SEM image, sample P1/14). **4** *Florisphaera profunda* in the *circled area* (SEM image, sample P1/34). **5** *Discoaster* spp. (SEM image, sample P1/34). **6** *Florisphaera profunda* (SEM image, sample P1/34). **7**–**10** Typical calcareous nannofossil assemblage of the grey marls. **7** (SEM image, sample P1/67): *a Umbilicosphaera jafari*, *b* small *Gephyrocapsa* spp., *c* small *Reticulofenestra* spp., *d Scyphosphaera* spp., *e Reticulofenestra* sp. **8** Small *Gephyrocapsa* spp. (SEM image, sample P1/67). **9** Small *Gephyrocapsa* spp. (LM image, sample P1/67). **9** *Syracolithus dalmaticus* (holococcolith, SEM image, sample P1/67). **10** *Umbilicosphaera jafari* (SEM image, sample P1/67). **11** small *Reticulofenestra* spp. (SEM image, sample P1/67)

Quaternary sapropels (e.g., Castradori 1993; Negri et al. 1999a, b; Triantaphyllou et al. 2009a, b; 2010; Triantaphyllou 2014). It is evident that *F. profunda* is a reliable proxy of the nutricline–thermocline (Okada and Honjo 1973; Molfino and McIntyre 1990); thus, high relative abundances indicate stable stratification of the water column and low productivity in the surface layer (e.g., Castradori 1993; Beaufort et al. 2001). The *Helicosphaera* species show affinities with shallow, eutrophic, or hyposaline environments (Perch-Nielsen 1985; Dimiza et al. 2014), and higher fertility regions (Ziveri et al. 2004). In particular, *Helicosphaera sellii* has been observed forming monospecific layers in OC-rich sediments, and is probably a key species in Pliocene

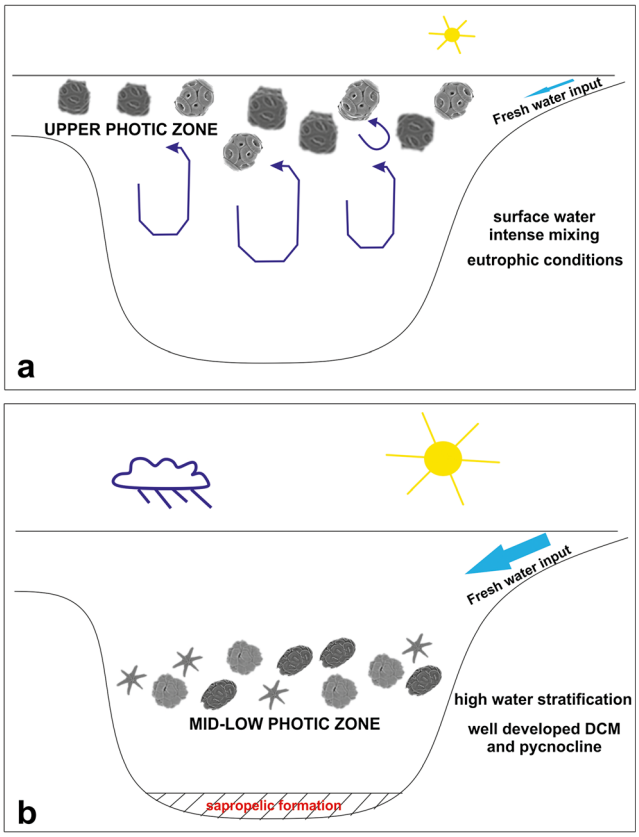

Fig. 9 Schematic representations of the palaeo-environmental conditions during the Zanclean/Piacenzian transition in Pissouri South sediments resulting to the formation of (**a**) grey marls, associated with intense mixing of the surface waters and development of eutrophic conditions in the upper photic zone during periods of low insolation and limited fresh water input in the basin, and (**b**) sapropelic layers, associated with high water column stratification, oligotrophic surface waters, nutrient increase in the mid-low photic zone and well-developed deep-chlorophyll maximum during periods of strong summer insolation and monsoonal maxima

sapropels, also related to high productivity in the mid photic zone (Capozzi et al. 2006). High values of the stratification S index have been reported in Quaternary sapropels of the Aegean (up to 0.9) and North Levantine Sea (>0.5), (Triantaphyllou 2014). Small peaks of reworked species within the laminated layers can be associated with increased fluvial discharge (e.g., Negri and Giunta 2001). In addition, higher values of discoasterids at the same levels are associated with oligotrophic surface waters. Discoasterids are generally considered to prefer warm waters (e.g., Flores et al. 1992; Vázque et al. 2000), increasing their abundance with deep pycnocline as lower photic zone inhabitants (Flores et al. 2005). Such conditions of marine biological production combined with enhanced organic matter preservation, are connected with sapropel formation during periods of wetter climate in the eastern Mediterranean and the Levantine Basin and the associated intense continental runoff, especially from the Nile, resulting from lower latitude monsoonal activity (e.g., Rohling and Hilgen 1991; Rohling 1994; Emeis et al. 1998; Bouloubassi et al. 1999; Warning and Brumsack 2000). Sapropels occurred in the entire eastern Mediterranean during intervals when the thermohaline circulation was reduced and the intermediate- and deep-water formation was weakened or impeded (Emeis et al. 1998).

Higher values of *F. profunda* have been previously documented in other Pliocene sapropels (Zanclean age) from the Mediterranean region (Castradori 1998), connecting the increased abundance of the species with the development of DCM. Similarly, Negri et al. (2003) observed the same pattern of a well-developed DCM favouring *F. profunda* during the deposition of Pleistocene sapropels. The subsequent shoaling of the pycnocline enables the upward mixing of new nutrients into the lower photic zone (the ecological niche of *F. profunda*), increasing the export of organic matter (e.g., Legendre and Le Fevre 1989; Eppley 1989). Apparently, this process relates the abundance of *F. profunda* with increased export of organic matter from the photic zone (e.g., Castradori 1998). Similar ecological affinities to those of the deep nutricline dweller *F. profunda* were also proposed for the Mesozoic taxon *Nannoconus* (e.g., Coccioni et al. 1992; Erba 1994); Street and Bown (2000), on the other hand, suggested that nannoconids were neritic, warm water, and r-selected taxa. Nannoconids experienced a profound crisis, whereas shallow dweller coccolithophores continued to bloom (e.g., Erba 2004; Erba and Tremolada 2004; Erba et al. 2010) just before the deposition of the Aptian grey–black anoxic shales of the Selli Level (Mesozoic possible analogues to the Cenozoic sapropels, e.g., Meyers and Negri 2003). Interestingly, Patruno et al. (2015) reported surface water conditions of high fertility and lowered pH featuring the onset of the anoxic Aptian Selli Level. Apparently, the deposition of these different anoxic layers displays contrasting features; concentration of nutrients in the upper photic zone during the Aptian global crisis vs nutrient increase in the deep photic zone during sapropel formation in the deep eastern Mediterranean basin. Despite all similarities observed between the Mesozoic black shales and the sapropels (e.g. Ryan and Cita 1977; Negri et al. 2003; Meyers and Negri 2003; Meyers 2006; Emeis and Weissert 2009), there are strong differences in their paleoenvironmental and paleoceanographic settings, mainly related to the presence of greenhouse conditions (black shales) vs glacial conditions (sapropels). In addition, as mentioned by Negri et al. (2003), there is no biotic evidence of DCM seen in the black shales, whereas presence of DCM is a common feature of the eastern Mediterranean Neogene sapropels, which is probably related to the high recorded abundances of *F. profunda*.

Pissouri South Pliocene sapropelic layers alternate with grey marls that are featured by the dominance of small placoliths of *Reticulofenestra* and *Gephyrocapsa* species (Figs. 8 and 9); *Reticulofenestra* spp. <5 μm and *Gephyrocapsa* spp. <3 μm are considered opportunistic taxa of the upper photic zone, indicating eutrophic conditions during intense mixing of the surface waters (Gartner 1988; Flores et al. 2005). In addition, Flores et al. (2005) argued that increased presence of small *Reticulofenestra* spp. is linked to a relatively shallow DCM, with a stable but also shallow thermocline. The presence, even in low abundances, of UPZ species in the grey marls (Fig. 5) supports relatively increased temperatures in the surface waters; Rhabdosphaeraceae, *Syracosphaera* spp., and *Pontosphaera* spp. prefer warm and oligotrophic waters (Okada and McIntyre 1979; Ziveri et al. 2004; Triantaphyllou et al. 2004; Dimiza et al. 2008; Malinverno et al. 2009). A similar pattern was also observed for *U. jafari* and holoccocolith distribution (Fig. 5), possibly reflecting time intervals of salinity increase (Flores et al. 2005; Wade and Bown 2006).

Our calcareous nannofossil assemblages support in general the prevalence of warm paleoclimatic conditions during the Zanclean/Piacenzian transition. However, the significant increase of the cold indicator *P. lacunosa*, observed between ~3.6–3.4 Ma (Fig. 4), is probably linked to slight sea surface temperature decrease, as the extinct species *P. lacunosa* is assumed by Flores et al. (1995) to suggest cool oceanographic conditions. The prevalence of cooler conditions, especially at ~ 3.35 Ma, is marked by the sharp peak of eutrophic small *Gephyrocapsa* spp. (Fig. 4), and the relatively reduced values of the warm UPZ taxa (Fig. 5). This cooling event can be correlated with the Mammoth cooling (Haug and Tiedemann 1998) that has been reported by several authors to represent the glacial MIS M2 at ~ 3.3. Ma (e.g., Lisiecki and Raymo 2005; De Schepper et al. 2009, 2013). However the increase of the lower and mid photic zone dwellers *F. profunda* and *H. sellii* and the high values of S index at 3.3 Ma (Fig. 4) support a mild expression of the glacial MIS M2 in the southeastern Mediterranean during generally warm climatic conditions.

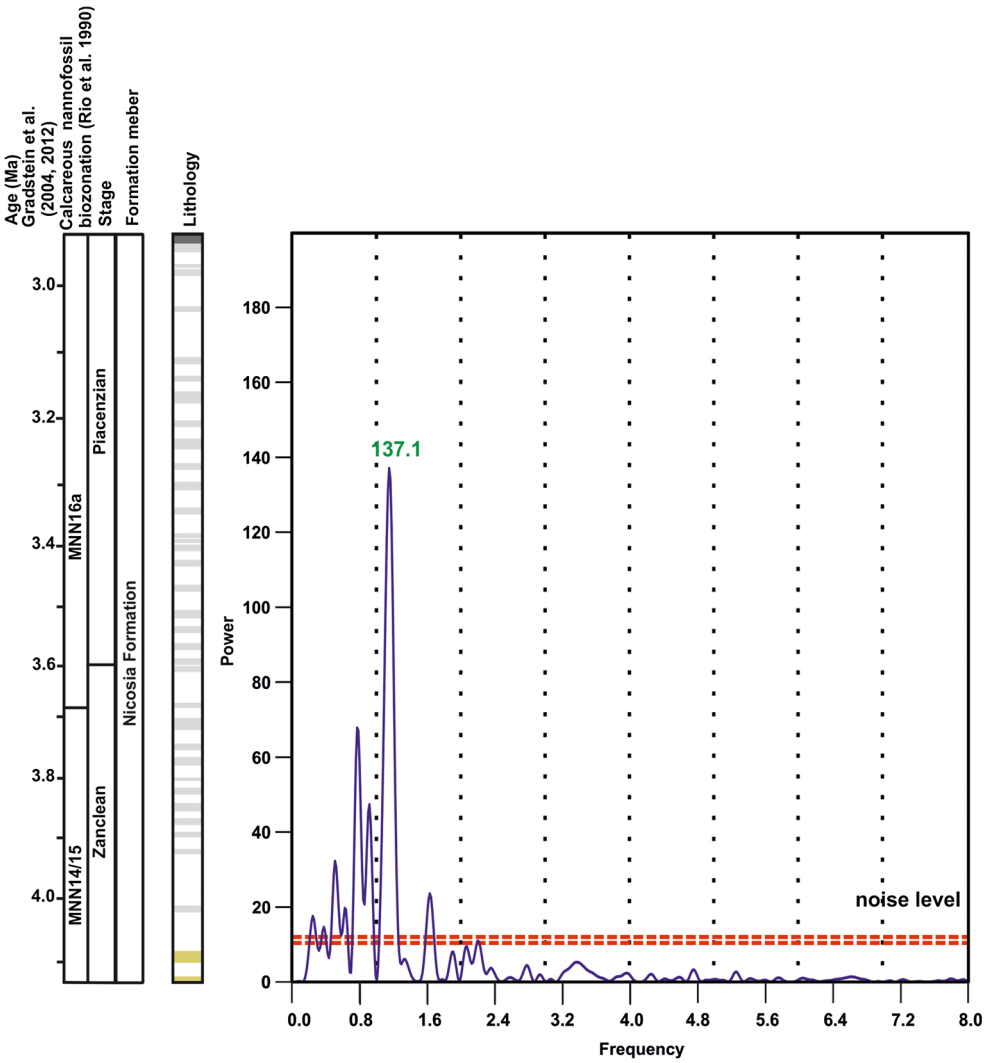

Fig. 10 Power analyses of the lithological rythmical alternations between 3.97 and 3.84 Ma in the Zanclean dated part of Pissouri South section

Cyclicity patterns, astronomical calibration, and provided age model

In order to provide new evidence on both age control and climatic variability for the Pliocene record of the Pissouri South section, we investigated the cyclic nature of the exposed lithological alternations between the organic-rich laminated layers and the grey marls. Therefore, we followed the approach of Mitchell et al. (2008) and Patruno et al. (2015) for a spectral analysis of the collected lithostratigraphic data covering the lowest part of the section spanning the time interval between 3.97 Ma and 3.84 Ma (10.2–15.8 m; Fig. 10, Table 1) within MNN14–MNN15 biozone, using Past.exe software. The aim of this investigation is to determine the main periodicities and the phase relationships relative to the astronomical forcing to our data. The results display an evident peak (11 times stronger than the noise level) with a period of 137 cm. The value of biostratigraphically-constrained

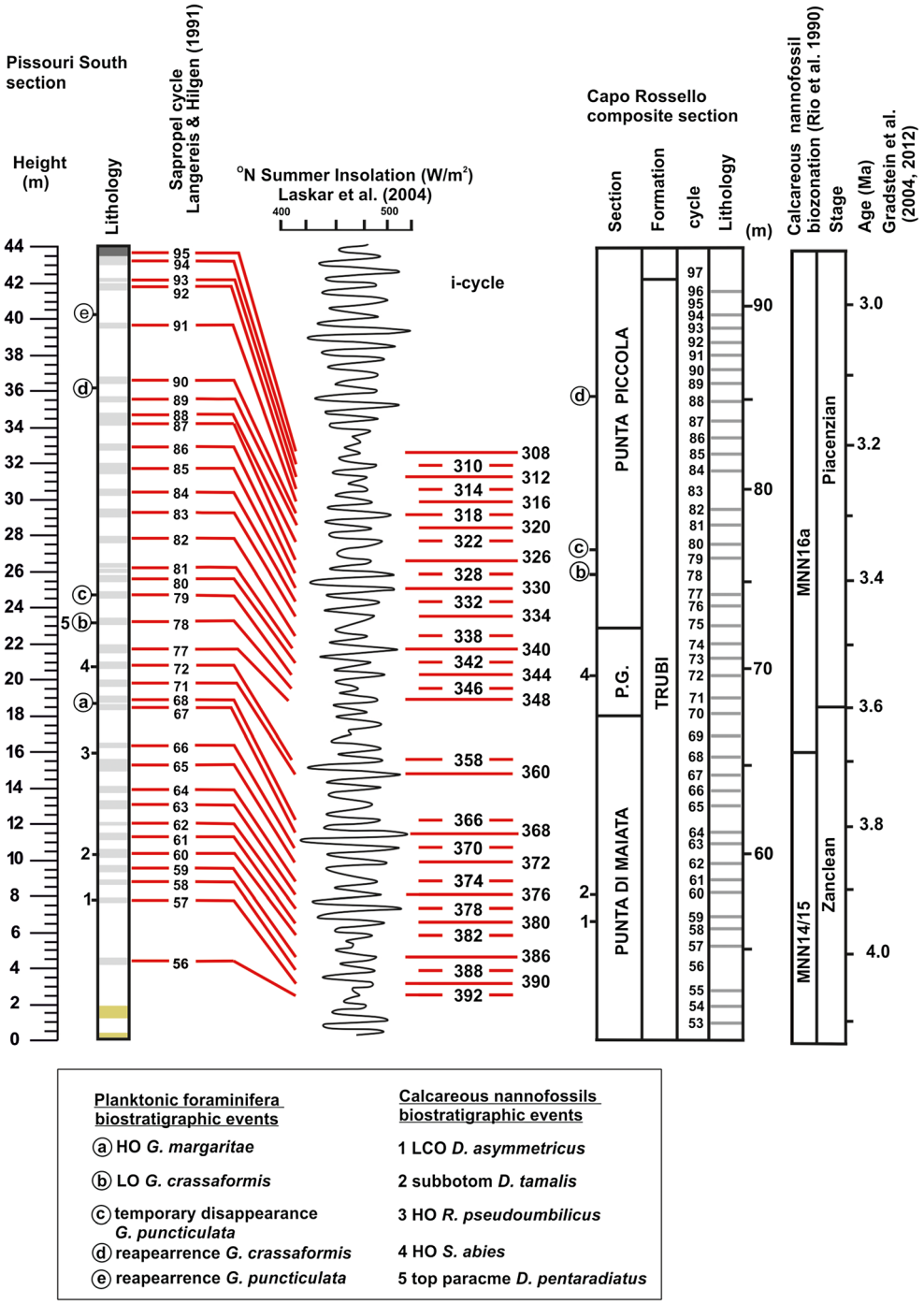

Fig. 11 Astronomical calibration of Pissouri South section. Sapropel cycles (highlighted in *grey bands*) are labelled according to i-cycle coding after Hilgen (1991b) and correlated to the 65°N summer insolation target-curve of Laskar et al. (2004). Biostratigraphic framework according to Rio et al. (1990), ages after Gradstein et al. (2012). Nannofossil biostratigraphic events are labelled as *1–5* and planktonic foraminifera biostratigraphic events (Triantaphyllou et al. 2010) are labelled (*a*)-(*e*). Correlation with Capo Rossello composite section marking the position of the main calcareous nannofossil (Lourens et al. 2004) and planktonic foraminifera bioevents (Sprovieri et al. 2006) is also shown

sedimentation rates in this part of the section is of ~4.2 cm/kyear (Table 1. As a consequence, these cycles represent periods of ca. 21–23 kyr and can be assumed to reflect orbital precession, consistent with the 'bundling cyclicity' described in other Early Pliocene records in the Mediterranean such as Trubi formation (5.4–3.3 Ma) of the Capo Rossello composite section (Hilgen 1991a, b; Thunell et al. 1991a, b; Lourens et al. 1996).

The available biostratigraphical framework for Pissouri South sediments provides an excellent first-order bed-to-bed age control through the comparison with the Rossello composite section, Sicily (Langereis and Hilgen 1991; Lourens et al. 1996), enabling the astronomical tuning of the marly–sapropelic cycles to the target-curve of Laskar et al. (2004), (Fig. 11). Approximate age for each insolation cycle for the Pissouri South section follows Laskar et al. (2004) and Lourens et al. (1996) calibrations. Thus, LCO *D. asymmetricus* at 7.7 m corresponds to Rossello sapropel cycle 57 (Fig. 11), which is tuned to i-cycle 390 (4.048 Ma). Sapropel cycle 56 is the lowest recorded at Pissouri South section, correlated with i-cycle 392; therefore, the studied sequence is astronomically dated younger than 4.065 Ma (Lourens et al. 1996). Subbottom *D. tamalis* reported within a sapropelic layer at 10.2 m corresponds to cycle 60 and i-cycle 382 (3.973 Ma). Sapropels 69–71 (i-cycles 364–360) and 73–76 (i-cycles 356–350) are not clearly recorded in the lithology of the studied sequence, most probably due to low sampling resolution at the specific interval and/or post-depositional diagenetic erasion (Emeis et al. 2000b). In between 18.9 m and 22.8 m, cycle 72 (20.6 m) corresponding to i-cycle 358 (3.702 Ma) was identified, associated with *Sphenolithus* spp. HO at 3.7 Ma (Table 1, Fig. 11). The interval 22.8–43 m presents a straightforward correlation between sapropel cycles 77–95 and i-cycles 348–308 (3.608–3.217 Ma); therefore, the top of the studied interval ends at 3.217 Ma (i-cycle 308; Lourens et al. 1996), (Fig. 11).

Conclusions

The main conclusions of our study can be summarized as following:

- Pissouri South sediments expose cyclical lithological alternations between organic-rich laminated layers and grey marls, reflecting the orbital precession. The provided biostratigraphical framework indicates the correlation with MNN14/15 and MNN16 calcareous nannofossil biozones, spanning the Zanclean/Piacenzian boundary. According to the astronomical tuning of the marly-sapropelic cycles, the studied section is dated between 4.065 Ma and 3.217 Ma.
- The provided evidence from Pissouri South section in southwestern Cyprus shows that during the Zanclean/Piacenzian transition, the paleoceanographic conditions indicated rhythmic alternations between sapropelic depositional intervals with high water column stratification associated with the increased values of *F. profunda*, and eutrophic conditions during mixing of the surface waters, featured by the dominance of small placoliths of *Reticulofenestra* and *Gephyrocapsa* species.
- Calcareous nannofossil assemblages support in general the prevalence of warm paleoclimatic conditions. The prevalence of cooler conditions, especially at~3.35 Ma, is marked by the sharp peak of eutrophic small *Gephyrocapsa* spp. is correlated with the Mammoth cooling (glacial MIS M2 at~3.3 Ma). The simultaneous increase of the lower and mid photic zone dwellers *F. profunda* and *H. sellii* and the high values of S index within sapropel cycle 91 at~3.3 Ma, support a mild expression of MIS M2 in the southeastern Mediterranean.
- Our data indicate relatively warm climate conditions during ~4.1–3.2 Ma in the southeastern Mediterranean, suggesting that this part of the basin was either decoupled from or not sensitive to the North Atlantic climate forcing (e.g., Becker et al. 2005; Wang et al. 2010). Apparently, southeastern Mediterranean's latitudinal position in combination with its limited connection to the open ocean, places the entire area under the influence of both temperate climate conditions and the African monsoon, which subsequently resulted to sapropel formation during the Zanclean/Piacenzian transition.

Acknowledgments This work has been made possible thanks to the financial support provided by EU EraNet/Marinera Medecos project and University of Athens, SARG 70/4/11078. Field work funding has been provided by Research Projects 70/3/7093 and 70/4/3570 financed by Cyprus Geological Survey and University of Athens, SARG. We are grateful to Dr. Efthimios Tsiolakis (Geological Survey of Cyprus) for his warm support during the field work. Critical comments by Stefano Patruno, Agata Di Stefano, and the journal editors have proved invaluable in improving the manuscript.

Conflict of interest The authors declare that they have no conflict of interest.

References

Aubry MP (1984) Handbook of Cenozoic calcareous nannoplankton: book 1, Ortholithae (*Discoaster*). Micropal Press, New York, pp 1–263

Aubry MP (1988) Handbook of Cenozoic calcareous nannoplankton: book 2, Ortholithae (Holococcoliths, Ceratoliths, Ortholiths and other). Micropal Press, New York, pp 1–279

Aubry MP (1989) Handbook of Cenozoic calcareous nannoplankton: book 3, Ortholithae (Pentaliths and other), Heliolithae

(Fasciculiths, Sphenoliths and others). Micropal Press, New York, pp 1–279

Aubry MP (1990) Handbook of Cenozoic calcareous nannoplankton: book 4, Heliolithae (Helicoliths, Cribriliths, Lopadoliths and other). Micropal Press, New York, pp 1–381

Aubry MP (2014) Cenozoic Coccolithophores, Discoasterales. Micropal Press, New York, pp 1–384

Backman J, Raffi I, Rio D, Fornaciari E, Pälike H (2012) Biozonation and biochronology of Miocene through Pleistocene calcareous nannofossils from low and middle latitudes. Newslett Strat 45: 221–244

Bar-Matthews M, Ayalon A, Kaufman A (2000) Timing and hydrological conditions of sapropel events in the eastern Mediterranean, as evident from speleothems, Soreq Cave, Israel. Chem Geol 169:145–156

Bartoli G, Hönisch B, Zeebe RE (2011) Atmospheric CO2 decline during the Pliocene intensification of Northern Hemisphere glaciations. Paleoceanography 26, PA4213

Beaufort L, De Garidel-Thoron T, Mix AC, Pisias NG (2001) ENSO-like forcing on oceanic primary production during the late Pleistocene. Science 293:2440–2444

Becker J, Lourens LJ, Hilgen FJ, Evd L, Kouwenhoven TJ, Reichart GJ (2005) Late Pliocene climate variability on Milankovitch to millennial time scales: a high-resolution study of MIS100 from the Mediterranean. Palaeogeogr Palaeoclimatol Palaeoecol 228:338–360

Beltran C, de Rafélis M, Minoletti F, Renard M, Sicre MA, Ezat U (2007) Coccolith δ 18O and alkenone records in middle Pliocene orbitally controlled deposits: high frequency temperature and salinity variations of sea surface water. Geochem Geophys Geosyst 8. doi:10.1029/2006GC001483

Bertoni C, Cartwright JA (2007) Major erosion at the end of the Messinian Salinity Crisis: evidence from the Levant Basin, eastern Mediterranean. Basin Res 19:1–18

Bison KM, Versteegh GJM, Orszag-Sperber F, Rouchy JM, Willems H (2009) Palaeoenvironmental changes of the early Pliocene (Zanclean) in the eastern Mediterranean Pissouri Basin (Cyprus) evidenced from calcareous dinoflagellate cyst assemblages. Mar Micropaleontol 73:49–56

Blanc-Valleron MM, Rouchy JM, Pierre C, Badaut-Trauth D, Schuler M (1998) Evidence of Messinian non-marine deposition at site 968 (Cyprus Lower Slope). Proc Ocean Drill Program Sci Res 160: 437–445

Bouloubassi I, Rullkötter J, Meyers PA (1999) Origin and transformation of organic matter in Pliocene–Pleistocene Mediterranean sapropels: Organic geochemical evidence reviewed. Mar Geol 153:177–197

Bown PR, Young JR (1998) Techniques. In: Bown PR (ed) Calcareous Nannofossil Biostratigraphy. Chapman and Hall, Kluwer Academic, pp 16–28

Brierley C, Fedorov AV, Liu Z, Herbert TD, Lawrence KT, LaRiviere JP (2009) Greatly expanded tropical warm pool and weakened Hadley Circulation in the Early Pliocene. Science 323:1714–1718

Capozzi R, Dinelli E, Negri A, Picotti V (2006) Productivity-generated annual laminae in mid-Pliocene sapropels deposited during precessionally forced periods of warmer Mediterranean climate. Palaeogeogr Palaeoclimatol Palaeoecol 235:208–222

Casford JSL, Rohling EJ, Abu-Zied RH, Fontanier C, Jorissen FJ, Leng MJ, Schmiedl G, Thomson J (2003) A dynamic concept for eastern Mediterranean circulation and oxygenation during sapropel formation. Palaeogeogr Palaeoclimatol Palaeoecol 190:103–119

Castradori D (1993) Calcareous nannofossil and the origin of Eastern Mediterranean sapropels. Paleoceanography 8:459–471

Castradori D (1998) Calcareous nannofossils in the basal Zanclean of the eastern Mediterranean Sea: remarks on paleoceanography and sapropel formation. Proc Ocean Drill Program Sci Results 160:113–123

Clark PU, Alley RB, Pollard D (1999) Northern Hemisphere ice-sheet influences on global climate change. Science 286:1104–1111

Coccioni R, Erba E, Premoli-Silva I (1992) Barremian–Aptian calcareous plankton biostratigraphy from the Gorgo a Cerbara section (Marche, central Italy) and implication for plankton evolution. Cret Res 13: 457–467

De Kaenel E, Villa G (1996) Oligocene-Miocene calcareous nannofossil biostratigraphy and paleoecology from the Iberia abyssal plain. Proc Ocean Drill Program Sci Results 149:79–105

De Lange GJ, Ten Haven HL (1983) Recent sapropel formation in the eastern Mediterranean. Nature 305:797–798

De Lange GJ, Thomson J, Reitz A, Slomp CP, Principato MS, Erba E, Corselli C (2008) Synchronous basin-wide formation and redox-controlled preservation of a Mediterranean sapropel. Nat Geosci 1: 606–610

De Schepper S, Head MJ, Groeneveld J (2009) North Atlantic Current variability through marine isotope stage M2 (circa 3.3 Ma) during the mid-Pliocene. Paleoceanography 24, PA4206

De Schepper S, Groeneveld J, Naafs BDA, Van Renterghem C, Hennissen J, Head MJ, Louwye S, Fabian K (2013) Northern Hemisphere glaciation during the globally warm early Late Pliocene. PLoS ONE 8(12):81508. doi:10.1371/journal.pone.0081508

Di Stefano A, Sturiale G (2010) Refinements of calcareous nannofossil biostratigraphy at the Miocene/Pliocene boundary in the Mediterranean region. Geobios 449:5–20

Di Stefano A, Verducci M, Lirer F, Ferraro L, Iaccarino SM, Hüsing SK, Hilgen FJ (2010) Paleoenvironmental conditions preceding the Messinian Salinity Crisis in the Central Mediterranean: integrated data from the Upper Miocene Trave section (Italy). Palaeogeogr Palaeoclimatol Palaeoecol 297:37–53

Di Stefano A, Foresi LM, Incarbona A, Sproveri M, Vallefuoco M, Iorio M, Pelosi N, Di Stefano E, Sangiorgi P, Budillon F (2015) Mediterranean Coccolithophore ecobiostratigraphy since the penultimate Glacial (the last 145,000 years) and ecobioevent traceability. Mar Micropaleontol 115:24–38

Dimiza MD, Triantaphyllou MV, Dermitzakis MD (2008) Seasonality and ecology of living coccolithophores in E. Mediterranean coastal environments (Andros Island, Middle Aegean Sea). Micropaleontology 54:159–175

Dimiza MD, Triantaphyllou MV, Malinverno E (2014) New evidence for the ecology of *Helicosphaera carteri* in polluted coastal environments (Elefsis Bay, Saronikos Gulf, Greece). J Nannoplankton Res 34:37–43

Dowsett HJ, Robinson MM, Haywood AM, Hill DJ, Dolan AM, Stoll DK, Chan WL, Abe-Ouchi A, Chandler MA, Rosenbloom NA, Otto-Bliesner BL, Bragg FJ, Lunt DJ, Foley KM, Riesselman CR (2012) Assessing confidence in Pliocene sea surface temperatures to evaluate predictive models. Nat Clim Chang 2:365–371

Driever BWM (1981) A quantitative study of Pliocene associations of *Discoaster* from the Mediterranean. Proc Kon Ned Akad Wet 84: 437–455

Emeis KC, Weissert H (2009) Tethyan–Mediterranean organic carbon-rich sediments from Mesozoic black shales to sapropels. Sedimentology 56:247–266

Emeis KC, Schulz HM, Struck U, Sakamoto T, Doose H, Erlenkeuser H, Howell M, Kroon D, Paterne M (1998) Stable isotope and alkenone temperature records of sapropels from sites 964 and 967: Constraining the physical environment of sapropel formation in the eastern Mediterranean Sea. Proc Ocean Drill Program Sci Res 60:309–331

Emeis KC, Struck U, Schulz HM, Bernasconi S, Sakamoto T, Martinez-Ruiz F (2000a) Temperature and salinity of Mediterranean Sea surface waters over the last 16,000 years: constraints on the physical environment of S1 sapropel formation based on stable oxygen isotopes and alkenone unsaturation ratios. Palaeogeogr Palaeoclimatol Palaeoecol 158:259–280

Emeis KC, Sakamoto T, Wehausen R, Brumsack HJ (2000b) The sapropel record of the eastern Mediterranean Sea — results of Ocean Drilling Program Leg 160. Palaeogeogr Palaeoclimatol Palaeoecol 158:371–395

Emeis KC, Schulz H, Struck U, Rossignol-Strick M, Erlenkeuser H, Howell MW, Kroon D, Mackensen H, Ishizuka S, Oba T, Sakamoto T, Koizumi I (2003) Eastern Mediterranean surface water temperatures and d18O composition during deposition of sapropels in the late Quaternary. Paleoceanography 18(1):1–18

Eppley RW (1989) New production: history, methods, problems. In: Berger WH, Smetacek VS, Wefer G (eds) Productivity of the ocean: present and past. John Wiley, Hoboken, pp 85–97

Erba E (1994) Nannofossils and superplumes: the Early Aptian "nannoconid crisis". Palaeoceanography 9:483–501

Erba E (2004) Calcareous nannofossils and Mesozoic oceanic anoxic events. Mar Micropaleontol 52:85–106

Erba E, Tremolada F (2004) Nannofossil carbonate fluxes during the Early Cretaceous: phytoplankton response to nutrification episodes, atmospheric CO_2, and anoxia. Paleoceanography 19(1):PA1008 1–18

Erba E, Bottini C, Weissert H, Keller CE (2010) Calcareous nannoplankton response to surface-water acidification around Oceanic Anoxic Event 1a. Science 329:428–432

Fenner J, Di Stefano A (2004) Late quaternary oceanic fronts along Chatham Rise indicated by phytoplankton assemblages, and refined calcareous nannofossil stratigraphy for the Mid-Latitude SW Pacific. Mar Geol 205:59–86

Flores JA, Sierro FJ, Glaçon G (1992) Calcareous plankton analysis in the pre-evaporitic sediments of the ODP site 654 (Tyrrhenian Sea, Western Mediterranean). Micropaleontology 38:279–288

Flores JA, Sierro FJ, Raffi I (1995) Evolution of the calcareous nannofossil assemblage as a response to the paleoceanographic changes in the Eastern Equatorial Pacific from 4 to 2 Ma (Leg 138, Sites 849 and 852). In: Pisias N et al (eds) Proceedings ODP, Science Results, Vol. 138. Ocean Drilling Program Publications, College Station, TX, pp 163–176

Flores JA, Bárcena MA, Sierro FJ (2000) Ocean-surface and wind dynamics in the Atlantic Ocean off Northwest Africa during the last 140,000 years. Palaeogeogr Palaeoclimatol Palaeoecol 161:459–478

Flores JA, Marino M, Sierro FJ, Hodell DA, Charles CD (2003) Calcareous plankton dissolution pattern and coccolithophore assemblages during the last 600 kyr at ODP Site 1089 (Cape Basin, South Atlantic): paleoceanographic implications. Palaeogeog Palaeoclimatol Palaeoecol 196:409–426

Flores JA, Sierro FJ, Filippelli GM, Bárcena MA, Pérez-Folgado M, Vázquez A, Utrilla R (2005) Surface water dynamics and phytoplankton communities during deposition of cyclic late Messinian sapropel sequences in the western Mediterranean. Mar Micropaleontol 56:50–79

Foucault A, Mélières F (2000) Palaeoclimatic cyclicity in central Mediterranean Pliocene sediments: the mineralogical signal. Palaeogeogr Palaeoclimatol Palaeoecol 158:311–323

Gartner S (1988) Paleoceanography of the Mid-Pleistocene. Mar Micropaleontol 13:23–46

Gogou A, Bouloubassi I, Lykousis V, Arnaboldi M, Gaitani P, Meyers PA (2007) Organic geochemical evidence of abrupt late Glacial–Holocene climate changes in the North Aegean Sea. Palaeogeogr Palaeoclimatol Palaeoecol 256:1–20

Gradstein FM, Ogg JG, Smith AG (2004) A geologic time scale 2004. Cambridge University Press, Cambridge UK, pp 589

Gradstein FM, Ogg JG, Schmitz MD, Ogg GM (2012) The geologic time scale 2012. Elsevier, Amsterdam, pp 1144

Harrison RW, Newell WL, Batihanli H, Panayides I, Mc Geehin JP, Mahan SA, Ozhur A, Tsiolakis E, Necdet M (2004) Tectonic framework and Late Cenozoic tectonic history of the northern part of Cyprus: implications for earthquake hazards and regional tectonics. J Asian Earth Sci 23:191–210

Haug GH, Tiedemann R (1998) Effect of the formation of the isthmus of Panama on Atlantic thermohaline circulation. Nature 393:673–676

Haywood AM, Valdes PJ (2004) Modelling Pliocene warmth: contribution of atmosphere, oceans and cryosphere. Earth Planet Sci Lett 218:363–377

Haywood AM, Hill DJ, Dolan AM, Otto-Bliesner BL, Bragg F, Chan WL, Chandler MA, Contoux C, Dowsett HJ, Jost A, Kamae Y, Lohmann G, Lunt DJ, Abe-Ouchi A, Pickering SJ, Ramstein G, Rosenbloom NA, Salzmann U, Sohl L, Stepanek C, Ueda H, Yan Q, Zhang Z (2013) Large-scale features of Pliocene climate: results from the Pliocene Model Intercomparison Project. Clim Past 9:191–209

Head MJ, Gibbard PL (2005) Early-middle Pleistocene transitions: an overview and recommendation for the defining boundary. In: Head MJ, Gibbard PL (eds) Early-Middle Pleistocene Transitions: The Land–Ocean Evidence. Geological Society Special Publications, London 247:1–18

Hilgen FJ (1991a) Astronomical calibration of Gauss to Matuyama sapropels in the Mediterranean and implication for geomagnetic polarity time scale. Earth Planet Sci Lett 104:226–244

Hilgen FJ (1991b) Extension of the astronomically calibrated (polarity) time scale to the Miocene/Pliocene boundary. Earth Planet Sci Lett 104:349–368

Hilgen FJ, Krijgsman W, Langereis CG, Lourens LJ, Santarelli A, Zachariasse WJ (1995) Extending the astronomical (polarity) time scale into the Miocene. Earth Planet Sci Lett 136:495–510

Hilgen FJ, Iaccarino S, Krijgsman W, Villa G, Langereis CG, Zachariasse WJ (2000) The Global Boundary Stratotype Section and Point (GSSP) of the Messinian Stage (uppermost Miocene). Episodes 23:172–178

Hsü KJ, Montadert L, Bernoulli D, Cita MB, Erickson A, Garrison RE, Kidd RB, Melieres F, Müller C, Wright R (1977) History of the Mediterranean salinity crisis. Nature 267:399–403

Kallel N, Paterne M, Labeyrie L, Duplessy JC, Arnold M (1997) Temperature and salinity records of the Tyrrhenian Sea during the last 18,000 years. Palaeogeogr Palaeoclimatol Palaeoecol 135:97–108

Kallel N, Duplessy JC, Labeyrie L, Fontugne M, Paterne M, Montacer M (2000) Mediterranean pluvial periods and sapropel formation over the last 200,000 years. Palaeogeogr Palaeoclimatol Palaeoecol 157:45–58

Katsouras G, Gogou A, Bouloubassi I, Emeis KC, Triantaphyllou MV, Roussakis G, Lykousis V (2010) Organic carbon distribution and isotopic composition in three records from the eastern Mediterranean Sea during the Holocene. Org Geochem 41:935–939

Kouli K, Gogou A, Bouloubassi I, Triantaphyllou MV, Chr I, Katsouras G, Roussakis G, Lykousis V (2012) Late postglacial paleoenvironmental change in the northeastern Mediterranean region: combined palynological and molecular biomarker evidence. Quat Internat 261:118–127

Kouwenhoven TJ, Morigi C, Negri A, Giunta S, Krijgsman W, Rouchy JM (2006) Paleoenvironmental evolution of the eastern Mediterranean during the Messinian: Constraints from integrated microfossil data of the Pissouri Basin (Cyprus). Mar Micropaleontol 60:17–44

Krijgsman W, Blanc-Valleron MM, Flecker R, Hilgen FJ, Kouwenhoven TJ, Merle D, Orszag-Sperber F, Rouchy JM (2002) The onset of the Messinian salinity crisis in the eastern Mediterranean (Pissouri Basin, Cyprus). Earth Planet Sci Let 194:299–310

Kroon D, Alexander I, Little M, Lourens LJ, Matthewson A, Robertson AHF, Sakamoto T (1998) Oxygen isotope and sapropel stratigraphy in the Eastern Mediterranean during the last 3.2 million years. Proc ODP 160:181–189

Kuhnt T, Schmiedl G, Ehrmann W, Hamann Y, Andersen N (2008) Stable isotopic composition of Holocene benthic foraminifers from the Eastern Mediterranean Sea, Past changes in productivity and deep water oxygenation. Palaeogeogr Palaeoclimatol Palaeoecol 268: 106–115

Langereis CG, Hilgen FJ (1991) The Rossello composite: a Mediterranean and global reference section for the Early to early Late Pliocene. Earth Planet Sci Lett 104:211–225

LaRiviere JP, Ravelo AC, Crimmins A, Dekens PS, Ford HL, Lyle M, Wara MW (2012) Late Miocene decoupling of oceanic warmth and atmospheric carbon dioxide forcing. Nature 486:97–100

Laskar J, Robutel P, Joutel F, Gastineau M, Correia ACM, Levrard B (2004) A long term numerical solution for the insolation quantities of the Earth. Astron Astrophys 428:261–285

Legendre L, Le Fevre J (1989) Hydrodynamical singularities as controls of recycled versus export production in oceans. In: Berger WH, Smetacek VS, Wefer G (eds) Productivity of the ocean: present and past. John Wiley, Hoboken, pp 49–63

Lisiecki LE, Raymo ME (2005) A Pliocene–Pleistocene stack of 57 globally distributed benthic $\delta^{18}O$ records. Paleoceanography 20, PA1003

Lisiecki LE, Raymo ME (2007) Plio–Pleistocene climate evolution: trends and transitions in glacial cycle dynamics. Quat Sci Rev 26: 56–169

Lourens LJ, Hilgen FJ, Gudjonsson L, Zachariasse WJ (1992) Late Pliocene to Early Pleistocene astronomically forced sea surface productivity and temperature variations in the Mediterranean. Mar Micropaleontol 19:49–78

Lourens LJ, Antonarakou A, Hilgen FJ, Van Hoof AAM, Vergnaud-Grazzini C, Zachariasse WJ (1996) Evaluation of the Plio–Pleistocene astronomical timescale. Paleoceanography 11(4):391–413

Lourens LJ, Hilgen FJ, Shackleton NJ, Laskar J, Wilson D (2004) Chapter 21: The Neogene Period. In: Gradstein F, Ogg I, Smith A (eds) A geological timescale 2004. Cambridge University Press, UK, pp 409–444

Malinverno E, Triantaphyllou MV, Stavrakakis S, Ziveri P, Lykousis V (2009) Seasonal and spatial variability of coccolithophore export production at the South-Western margin of Crete (Eastern Mediterranean). Mar Micropaleontol 71:131–147

Marlow JR, Lange CB, Wefer G, Rosell-Melé A (2000) Upwelling intensification as part of the Plio–Pleistocene climate transition. Science 290:2288–2291

Martini E (1971) Standard Tertiary and Quaternary calcareous nannoplankton zonation. In: Farinacci A (ed), Proc II Planktonic Conf Roma, pp 739–785

Mc Callum JE, Robertson AHF (1995) Sedimentology of two fan-delta systems in the Pliocene–Pleistocene of the Mesaoria Basin, Cyprus. Sed Geol 98:215–244

Meyers PA (2006) Paleoceanographic and paleoclimatic similarities between Mediterranean sapropels and Cretaceous black shales. Palaeogeogr Palaeoclimatol Palaeoecol 235:305–320

Meyers PA, Negri A (2003) Paleoclimatic and paleoceanographic records in Mediterranean sapropels and Mesozoic black shales. Palaeogeogr Palaeoclimatol Palaeoecol 190:1–480

Mitchell RN, Bice DB, Montanari A, Cleaveland L, Christianson KT, Coccioni R, Hinnov LA (2008) Oceanic anoxic cycles? Orbital prelude to the Bonarelli Level (OAE2). Earth Planet Sci Lett 267:1–16

Molfino B, McIntyre A (1990) Precessional forcing of nutricline dynamics in the equatorial Atlantic. Science 249:766–769

Morigi C, Negri A, Giunta S, Kouwenhoven T, Krijgsman W, Blanc-Valleron MM, Orszag-Sperber F, Rouchy JM (2007) Integrated quantitative biostratigraphy of the latest Tortonian–early Messinian Pissouri section (Cyprus): An evaluation of calcareous plankton bioevents. Geobios 40:267–279

Müller C (1985) Late Miocene to recent Mediterranean biostratigraphy and paleoenvironments based on calcareous nannoplankton. In: Stanley J, Wezel FC (eds) Geological evolution of the Mediterranean Basin. Springer-Verlag, New York, pp 471–485

Naafs BDA, Stein R, Hefter J, Khélifi N, De Schepper S, Haug GH (2010) Late Pliocene changes in the North Atlantic Current. Earth Planet Sci Lett 298:434–442

Negri A, Giunta S (2001) Calcareous nannofossil paleoecology in the sapropel S1 of the eastern Ionian Sea: paleoceanographic implications. Palaeogeogr Palaeoclimatol Palaeoecol 169:101–112

Negri A, Villa G (2000) Calcareous nannofossil biostratigraphy, biochronology and paleoecology at the Tortonian/Messinian boundary of the Faneromeni section (Crete). Palaeogeogr Palaeoclimatol Palaeoecol 156:195–209

Negri A, Capotondi L, Keller J (1999a) Calcareous nannofossils, planktonic foraminifera and oxygen isotopes in the late Quaternary sapropels of the Ionian Sea. Mar Geol 157:89–103

Negri A, Giunta S, Hilgen FJ, Krijgsman W, Vai GB (1999b) Calcareous nannofossil biostratigraphy of the M. del Casino section (northern Apennines, Italy) and paleoceanographic conditions at times of late Miocene sapropel formation. Mar Micropaleontol 36:13–30

Negri A, Cobianchi M, Luciani V, Fraboni R, Milani A, Claps M (2003) Tethyan Cenomanian pelagic rhythmic sedimentation and Pleistocene Mediterranean sapropels: is the biotic signal comparable? Palaeogeogr Palaeoclimatol Palaeoecol 190:373–397

Okada H, Honjo S (1973) The distribution of ocean coccolithophorids in the Pacific. Deep-Sea Res 20:355–374

Okada H, McIntyre A (1979) Seasonal distribution of modern coccolithophorids in the western North Atlantic Ocean. Mar Biol 54:319–328

Pagani M, Liu Z, LaRiviere J, Ravelo AC (2009) High Earth-system climate sensitivity determined from Pliocene carbon dioxide concentrations. Nat Geosci 3:27–30

Palumbo E, Flores JA, Perugia C, Petrillo Z, Voelker AHL, Amore FO (2013) Millennial scale coccolithophore paleoproductivity and surface water changes between 445 and 360 ka (Marine Isotope Stages 12/11) in the Northeast Atlantic. Palaeogeogr Palaeoclimatol Palaeoecol 383–384:27–41

Patruno S, Triantaphyllou MV, Erba E, Dimiza MD, Bottini C, Kaminski MA (2015) The Barremian and Aptian stepwise development of the 'Oceanic Anoxic Event 1a' (OAE 1a) crisis: Integrated benthic and planktic high-resolution palaeoecology along the Gorgo a Cerbara stratotype section (Umbria–Marche Basin, Italy). Palaeogeogr Palaeoclimatol Palaeoecol 424:147–182

Payne AS, Robertson AHF (1995) Neogene supra-subduction zone extension in the Polis graben system, West Cypus, J. Geol Soc London 152:613–628

Perch-Nielsen K (1985) Cenozoic calcareous nannofossils. In: Bolli HM, Saunders JB, Perch-Nielsen K (eds) Plankton stratigraphy. Cambridge University Press, Cambridge UK, pp 427–555

Raffi I, Backman J, Fornaciari E, Pälike H, Rio D, Lourens L, Hilgen F (2006) A review of calcareous nannofossil astrobiochronology encompassing the past 25 million years. Quat Sci Rev 25:3113–3137

Ravelo AC, Billups K, Dekens PS, Herbert TD, Lawrence KT (2007) On to the ice ages: proxy evidence for the onset of Northern Hemisphere glaciation. In: Williams M, Haywood AM, Gregory FJ, Schmidt DN (eds) Deep-time perspectives on climate change: marrying the signal from computer models and biological proxies. The Micropalaeontological Society, Spec Publ Geol Soc, London, pp 563–573

Rio D, Raffi I, Villa G (1990) Pliocene Pleistocene calcareous nannofossils distribution patterns in the western Mediterranean. Proc Ocean Drill Program Sci Res 107:513–533

Robertson AHF, Eaton S, Follows EJ, McCallum JE (1991) The role of local tectonics versus global sea-level change in the Neogene evolution of the Cyprus active margin. Spec Publ Intern Assoc Sedimentol 12:331–369

Rohling EJ (1994) Review and new aspects concerning the formation of eastern Mediterranean sapropels. Mar Geol 122:1–28

Rohling EJ, Hilgen FJ (1991) The eastern Mediterranean climate at times of sapropel formation: a review. Geol Mijn 70:253–264

Rohling EJ, Cane TR, Cooke S, Sprovieri M, Bouloubassi I, Emeis KC, Schiebel R, Kroon D, Jorissen FJ, Lorre A, Kemp AES (2002) African monsoon variability during the previous interglacial maximum. Earth Planet Sci Lett 202:61–75

Rohling EJ, Abu-Zied RH, Casford JSL, Hayes A, Hoogakker BAA (2009) The marine environment: present and past. In: Woodward JC (ed) The Physical geography of the Mediterranean. Oxford University Press, Oxford, pp 33–67

Rossignol-Strick M (1983) African monsoons, an immediate climate response to orbital insolation. Nature 304:46–49

Rossignol-Strick M (1985) Mediterranean Quaternary sapropels, an immediate response of the African monsoon to variation of insolation. Palaeogeogr Palaeoclimatol Palaeoecol 49:237–263

Roth PH, Coulbourn WT (1982) Floral and dissolution patterns of coccoliths in surface sediments of the North Pacific. Mar Micropaleontol 7:1–52

Rouchy JM, Orszag-Sperber F, Blanc-Valleron MM, Pierre C, Rivière M, Combourieu Nebout N, Panayides I (2001) Paleoenvironmental changes at the Messinian–Pliocene boundary in the eastern Mediterranean (Southern Cyprus basins): significance of the Messinian Lago-Mare. Sed Geol 145:93–117

Ryan WBF, Cita MB (1977) Ignorance concerning episodes of ocean-wide stagnation. Mar Geol 23:197–215

Schirmer W (2000) Neogene submarine relief and Troodos uplift in southeastern Cyprus. In: Panayides I, Xenophontos C, Malpas J (eds), Proceedings of the Third International Conference on the Geology of the Eastern Mediterranean, pp 125–134

Schmiedl G, Kuhnt T, Ehrmann W, Emeis KC, Hamann Y, Kotthoff U, Dulski P, Pross J (2010) Climatic forcing of eastern Mediterranean deep-water formation and benthic ecosystems during the past 22, 000 years. Quat Sci Rev 29:3006–3020

Sierro FJ, Flores JC, Civis J, González -Delgado JA, Francés G (1993) Late Miocene globorotaliid event-stratigraphy and biogeography in the NE Atlantic and Mediterranean. Mar Micropal 21:143–168

Sierro FJ, Flores JC, Francés G, Vazquez A, Utrilla R, Zamarrenõ I, Erlenkeuser H, Barcena MA (2003) Orbitally-controlled oscillations in planktic communities and cyclic changes in western Mediterranean hydrography during the Messinian. Palaeogeogr Palaeoclimatol Palaeoecol 190:289–316

Soria JM, Caracuel JE, Corbì H, Dinarès-Turell J, Lancis C, Tent-Manclùs J, Yébenes A (2008) The Bajo Segura Basin (SE Spain): implications for the Messinian Salinity Crisis in the Mediterranean margins. Stratigraphy 5:259–265

Sprovieri R, Di Stefano E, Incarbona A, Oppo DW (2006) Suborbital climate variability during Marine Isotopic Stage 5 in the central Mediterranean basin: evidence from calcareous plankton record. Quat Sci Rev 25:2332–2342

Stow DAV, Braakenburg NE, Xenophontos C (1995) The Pissouri Basin fan-delta complex, southwestern Cyprus. Sed Geol 98:245–262

Street C, Bown PR (2000) Paleobiogeography of Early Cretaceous (Berriasian–Barremian) calcareous nannoplankton. Mar Micropaleontol 39:265–291

Suc JP, Bertini A, Combourieu-Nebout N, Diniz F, Leroy S, Russo-Ermolli E, Zheng Z, Bessais E, Ferrier J (1995) Structure of West Mediterranean and climate since 5.3 Ma. Acta Zool Cracov 38:3–16

Thunell R, Rio D, Sprovieri R, Raffi I (1991a) Limestone-marl couplets: origin of the early Pliocene Trubi Marls in Calabria, southern Italy. J Sed Petrol 61:1109–1122

Thunell R, Rio D, Sprovieri R, Vergnaud-Grazzini C (1991b) An overview of the post-Messinian paleoenvironmental history of the western Mediterranean. Paleoceanography 6:143–163

Triantaphyllou MV (2014) Coccolithophore assemblages during the Holocene Climatic Optimum in the NE Mediterranean (Aegean and northern Levantine Seas, Greece): paleoceanographic and paleoclimatic implications. Quat Int 345:56–67

Triantaphyllou MV, Dimiza MD, Dermitzakis MD (2004) *Syracosphaera halldalii* and *Calyptrolithina divergens* var. *tuberosa* life-cycle association and relevant taxonomic remarks. Micropaleontology 50: 121–126

Triantaphyllou MV, Antonarakou A, Kouli K, Dimiza M, Kontakiotis G, Papanikolaou M, Ziveri P, Mortyn G, Lianou V, Lykousis V, Dermitzakis MD (2009a) Late Glacial–Holocene ecostratigraphy of the south-eastern Aegean Sea, based on plankton and pollen assemblages. Geo-Mar Lett 29:249–267

Triantaphyllou MV, Ziveri P, Gogou A, Marino G, Lykousis V, Bouloubassi I, Emeis KC, Kouli K, Dimiza M, Rosell-Mele A, Papanikolaou M, Katsouras G, Nunez N (2009b) Late Glacial–Holocene climate variability at the south-eastern margin of the Aegean Sea. Mar Geol 266:182–197

Triantaphyllou MV, Antonarakou A, Drinia H, Dimiza MD, Kontakiotis G, Tsiolakis E, Theodorou G (2010) High-resolution biostratigraphy and paleoecology of the early Pliocene succession of Pissouri Basin (Cyprus island). Bull Geol Soc Greece XLIII:763–772

Triantaphyllou MV, Gogou A, Bouloubassi I, Dimiza MD, Kouli K, Roussakis G, Kotthoff U, Emeis KC, Papanikolaou M, Athanasiou M, Parinos K, Ioakim C, Lykousis V (2013) Evidence for a warm and humid Mid-Holocene episode in the Aegean and northern Levantine Seas (Greece, NE Mediterranean). Reg Environ Chang 14:1697–1712

Vázque A, Utrilla R, Zamarrennõ I, Sierro FJ, Flores JA, Francés G (2000) Precession-related sapropels of the Messinian Sorbas Basin (south Spain): paleoenvironmental significance. Palaeogeogr Palaeoclimatol Palaeoecol 158:353–370

Wade BS, Bown PR (2006) Calcareous nannofossils in extreme environments: the Messinian salinity Crisis, Polemi Basin, Cyprus. Palaeogeogr Palaeoclimatol Palaeoecol 233:271–286

Wang P, Tian J, Lourens LJ (2010) Obscuring of long eccentricity cyclicity in Pleistocene oceanic carbon isotope records. Earth Planet Sci Lett 290:319–330

Warning B, Brumsack HJ (2000) Trace metal signatures of eastern Mediterranean sapropels. Palaeogeogr Palaeoclimatol Palaeoecol 158:293–309

Waters JV, Jones SJ, Armstrong HA (2010) Climatic controls on late Pleistocene alluvial fans, Cyprus. In: Wilford D, Nichols G, Giles P (eds), Alluvial fan research and management: from reconstructing past environments to identifying the contemporary hazards. Geomorphology 115:228–251

Ziveri P, Baumann KH, Böckel B, Bollmann J, Young J (2004) Biogeography of selected coccolithophores in the Atlantic Ocean, from Holocene sediments. In: Thierstein H, Young J (eds) Coccolithophores: from molecular processes to global impact. Springer, Berlin Heidelberg, pp 403–428